Quaternary Environments and Humans 2 (2024) 100011

Contents lists available at ScienceDirect

Quaternary Environments and Humans

journal homepage: www.journals.elsevier.com/quaternary-environments-and-humans

Ecology of large ungulates in the northeastern Iberian Peninsula during the Upper Palaeolithic through stable isotopes and tooth wear analysis

Dorothée G. Drucker[a,*], Florent Rivals[b,c,d], Jordi Nadal[e], Isaac Ruf[f], Joaquim Soler[f,g], Narcís Soler[f], Julià Maroto[f]

[a] Senckenberg Centre Human Evolution and Palaeoenvironment, University of Tübingen, Germany
[b] ICREA, Barcelona, Spain
[c] Institut Català de Paleoecologia Humana i Evolució Social (IPHES-CERCA), Tarragona, Spain
[d] University Rovira i Virgili, Departament d'Història i Història de l'Art, Tarragona, Spain
[e] SERP, University of Barcelona, Catalonia, Spain
[f] Institut de Recerca Històrica, Universitat de Girona, Catalonia, Spain
[g] Institut Català de Recerca en Patrimoni Cultural (ICRPC-CERCA), Girona, Catalonia, Spain

ARTICLE INFO

Keywords:
Horse
Red deer
Catalonia
Last Glacial Maximum
Refugium

ABSTRACT

The northeastern Iberian Peninsula acted as a refuge zone during the Late Pleistocene where the persistence of terrestrial ecosystems could provide hunter-gatherers with large prey, mainly horse (*Equus ferus*) and red deer (*Cervus elaphus*). Isotopic ($\delta^{13}C$, $\delta^{18}O$, $\delta^{15}N$) and dental wear (mesowear and microwear) analyses have been applied on the remains of both species from the archaeological sites of Arbreda and Bora Gran at Serinyà (Girona), where evidence of human occupation from the Mousterian to the Magdalenian has been attested. The incremental enamel analysis on horse teeth revealed seasonal variation in carbonate $\delta^{18}O$ but no detectable change in carbonate $\delta^{13}C$ values, reflecting a rather stable diet and habitat over the year. Nevertheless, higher inter-individual than intra-individual contrast in carbonate $\delta^{13}C$ indicate different environmental conditions from one individual to another for each stratigraphic unit. In red deer teeth, seasonal signals in enamel carbonate $\delta^{13}C$ and $\delta^{18}O$ demonstrated mirrored trends. Further, red deer show higher $\delta^{13}C$ values than those of horses, both in enamel carbonate and bone collagen, as well as higher variability in mesowear and microwear scores, reflecting a mixed-feeding habit. Despite a strong grazing signal in mesowear and microwear, the lower $\delta^{13}C$ values for horses suggest a higher dependence on relatively more humid habitats than red deer, which likely foraged in dryer environments with xeric plants during winter. These differences in ecological partitioning are particularly well illustrated in distinct collagen $\delta^{13}C$ and $\delta^{15}N$ values during the harsh climatic conditions of the Final Gravettian coeval to the GS-3 or Last Glacial Maximum. The capacity of red deer to adapt to fluctuating environmental conditions contrasts with the niche persistence of horse allowed by the availability of mosaic habitat.

1. Introduction

The occupation of Europe by humans during the Late Pleistocene (ca. 115,000–11,700 calibrated BP) was challenged by phases of climatic deterioration and glacial advances, which restricted the distribution of habitable ecosystems (e.g. Margari et al., 2023). Ice-core $\delta^{18}O$ records in Greenland, such as the North Greenland Ice Core Project (NGRIP), illustrate the high climate instability over the Marine Isotope Stage 3 (MIS-3; ca. 59,400–27,800 years cal BP) and MIS-2 (ca. 27,800–14,700 cal BP) at a global scale with high chronological resolution. The Last Glacial Maximum (LGM), here defined as equivalent with the GS-3 of the NGRIP record (Lowe et al., 2008; Hughes and Gibbard, 2015), witnessed the southward withdrawal of plants, animals, and humans in refugial regions encompassing the Iberian, Italian and Balkan peninsulas, as well as southern France (e.g. Banks et al., 2008; Sommer and Nadachowski, 2006; Svenning et al., 2008; Stewart et al., 2010). In these refugia, sustainable conditions for terrestrial organisms could persist despite fluctuating climatic conditions, before their northward re-expansion during the warming phases of the Lateglacial (ca. 14,700–11,700 cal BP) (e.g. Banks et al., 2008; Burke

* Corresponding author.
E-mail addresses: dorothee.drucker@senckenberg.de, dorothee.drucker@ifu.uni-tuebingen.de (D.G. Drucker).

https://doi.org/10.1016/j.qeh.2024.100011
Received 29 December 2023; Received in revised form 9 May 2024; Accepted 2 June 2024
Available online 5 June 2024

et al., 2018). In the Iberian Peninsula, an uninterrupted human presence is confirmed by numerous archaeological sites, with extended stratigraphic records in some cases (e.g. Straus et al., 2000). Genetic continuity among successive human groups throughout the LGM and the Lateglacial has also been demonstrated for this region (Fu et al., 2016; Posth et al., 2023), which thus played a crucial role in the persistence and survival of ecological niches in Europe.

The question of how climatic fluctuations impacted the local terrestrial context is of particular interest when dealing with a refugial region as in the case of the Iberian Peninsula. In the Mediterranean Iberian Peninsula, anthracological and palynological data from natural and archaeological contexts indicated a succession of cold coniferous forest replaced by open landscape composed of cold and dry adapted plants during the LGM, followed by woodland extension evolving from cool pine forest to a mix of evergreen and deciduous trees (e.g. Barton et al., 2013; Cascalheira et al., 2021). Besides these environmental indicators, mammal assemblages associated with anthropogenic activity have provided valuable insights into the conditions of human subsistence (e.g. Álvarez-Lao and García, 2010; Domingo et al., 2015; Jones et al., 2020). Zooarchaeological and stable isotopes evidences point to the high reliance of human groups on terrestrial resources during the MIS-3 and MIS-2, especially *Cervus elaphus*, *Capra pyrenaica* and *Equus ferus*, as main large game in Mediterranean Iberia in proportions differing with topography and time (e.g. Garcia-Guixé et al., 2009; Aura Tortosa et al., 2016; Straus, 2013; Drucker et al., 2021).

In this paper, we explore the ecological response of large herbivores exploited by human populations to the fluctuating environmental conditions in the northeastern Iberian Peninsula between ca. 55,000 and 15,000 cal BP. Exploitation of large-bodied herbivores impacts the hunting strategy and land-use, which in turn will influence human resilience to environmental changes (e.g. Barton et al., 2013). To this goal, we applied stable isotope and dental wear analysis on horses (*Equus ferus*) and red deer (*Cervus elaphus*), the primary large prey targeted by local hunter-gatherers. The northeastern Iberian Peninsula is located at the contact zone between the Euro-Siberian conditions prevailing north of the Pyrenees and the Mediterranean bioclimatic zone. Although the region acted as a refugium, environmental changes have been recorded through local indicators, such as pollen and lake level records (e.g. Höbig et al., 2012; Vegas-Vilarrúbia et al., 2013). We aim to decipher if the ecological flexibility of horses and red deer allowed them to adapt to changing conditions, or if they could maintain the same diets and habitats over time thanks to locally buffered climatic conditions.

2. Background

2.1. The Serinyà caves

2.1.1. Archaeological record

The Arbreda cave (42º 09' 04" N, 2º 44' 45" E), at 206 m over sea level, is located in the municipality of Serinyà, in NE Catalonia (Spain), between the middle range mountains of the Catalan Transversal Range and the Banyoles lacustrine system. The cave is close to other relevant Palaeolithic sites such as Reclau Viver, Pau, Cau del Roure, Mollet and Mollet III (Fig. 1), all of which are aligned along a 200-metre-long travertine cliff of waterfall origin known as the *Paratge de les coves del Reclau* (Soler, 1999; Maroto, 2014).

Arbreda cave has provided a remarkably long and continuous sequence of human occupation over more than 12 m of stratigraphy (Figure A.1–1), which comprise Middle (N-I) and Upper Palaeolithic (H-A) levels and a final *terra rossa* stratum with sparse Mesolithic and Neolithic finds that seal the site. The cave was discovered by Josep Maria Corominas, who, in 1972, began to excavate it. First, he excavated the northern edge of the site (Gamma sector), which only provided materials from the Neolithic and was quickly abandoned. Next to this first excavation, he opened a second test pit, which revealed nearly 9 m of deposits, including Upper and Middle Palaeolithic levels (Alpha sector). His results highlighted the importance of the Arbreda cave and, in 1975, the excavations were resumed and enlarged towards the south (Beta sector), where current excavations are ongoing.

The oldest recorded evidence in Arbreda cave corresponds to the Neanderthal occupations from the basal level N, dated around 120,000 cal BP. As in the case of levels M and L above, it has provided a rich collection of lithic and faunal remains with abundant evidence of human activity. In contrast, the subsequent Mousterian levels K, J and I, contain regular but sparse evidence of human occupations and an intense presence of ursids. The final Neanderthal occupations are represented by the Final Mousterian level I, the uppermost section of which has provided Chatelperronian points but no ornamental artefacts, bone tools or lithic blade industries. This Final Mousterian is immediately followed by the Protoaurignacian level H. The boundary between the two periods has been established by ultrafiltrated ^{14}C AMS dating and Bayesian modelling with OxCal between ca. 42,300 and 40,300 cal BP (Wood et al., 2014). The following Evolved Aurignacian level (G) represents one of the major periods of the Upper Palaeolithic sequence recorded in Arbreda cave, and contains two combustion structures.

The Gravettian period is represented by levels F, E and D. Level F is sparse in comparison to the above level E, which corresponds to the Iberian Middle Gravettian. The subsequent level D corresponds to the Final Gravettian, and it shows an increased density of finds and a wider horizontal extension. This Final Gravettian period is also well represented in the neighbouring sites of Mollet III and Reclau Viver, where the earliest *Homo sapiens* remains of the Upper Palaeolithic in the region have been authenticated (Soler et al., 2013; Drucker et al., 2021).

The Solutrean is also well represented in Arbreda, although the occupations are not widely sparse but mostly restricted to the northeastern areas of the cave, where preserved parts of its ceiling were found. Level C belongs to the Middle Solutrean, while level B corresponds to the Final Solutrean. This has been attested by the presence of Serinyadell points in level C, which consists of a bifacial leaf point with a diverted tang. In contrast, level B lacks bifacial, flat, retouched artefacts and has provided the expected small-shouldered points with abrupt retouching that are typical of the Mediterranean type.

Level A closes the Upper Palaeolithic sequence of Arbreda cave. In older publications, it appeared as "post palaeolithic" because it was only marginally excavated, and cultural evidence is lacking to correctly it to any particular period. Recent excavations have provided lithic and bone artefacts attributed to the Magdalenian (Soler et al., 2014), as confirmed by a ^{14}C AMS date of 13,700 ± 40 uncal BP (Soler et al., 2021).

The Bora Gran d'en Carreras site (42°10'23.86"N, 2°44'34.90"E, 175 m a.s.l.) is a wide rock-shelter located 1.4 km northwards from Arbreda cave (Soler, 1976). In comparison with Arbreda, Bora Gran has a more condensed stratigraphy and chronology. Bora Gran was the first Palaeolithic site excavated in Catalonia, initially by Edouard Harlé in 1882, who attributed the site to the Magdalenian following the opinion of Gabriel de Mortillet (Harlé, 1882) and shortly afterwards by Pere Alsius i Torrent, who recovered Magdalenian two-side barbeled harpoons and identified the presence or reindeer (Alsius, 2015). In 1907, Josep Bosoms resumed the excavation in Bora Gran and gathered a much larger collection than Harlé or Alsius (Pericot and Maluquer, 1951). At the time, the deposits of the site were considered exhausted. However, in 1930 and 1935, the brothers Josep Maria and Frederic Corominas recovered substantial materials after sieving the extracted sediments left by the previous excavations (Corominas, 1949). Finally, Lluís Pericot and Joan Maluquer excavated the site again in 1944 and 1945 (Pericot, 1945).

At the regional scale, the occupations of Bora Gran clearly come next to those documented in Arbreda cave, where the Magalenian occupation is scarce and does not contain harpoons. In contrast, harpoons

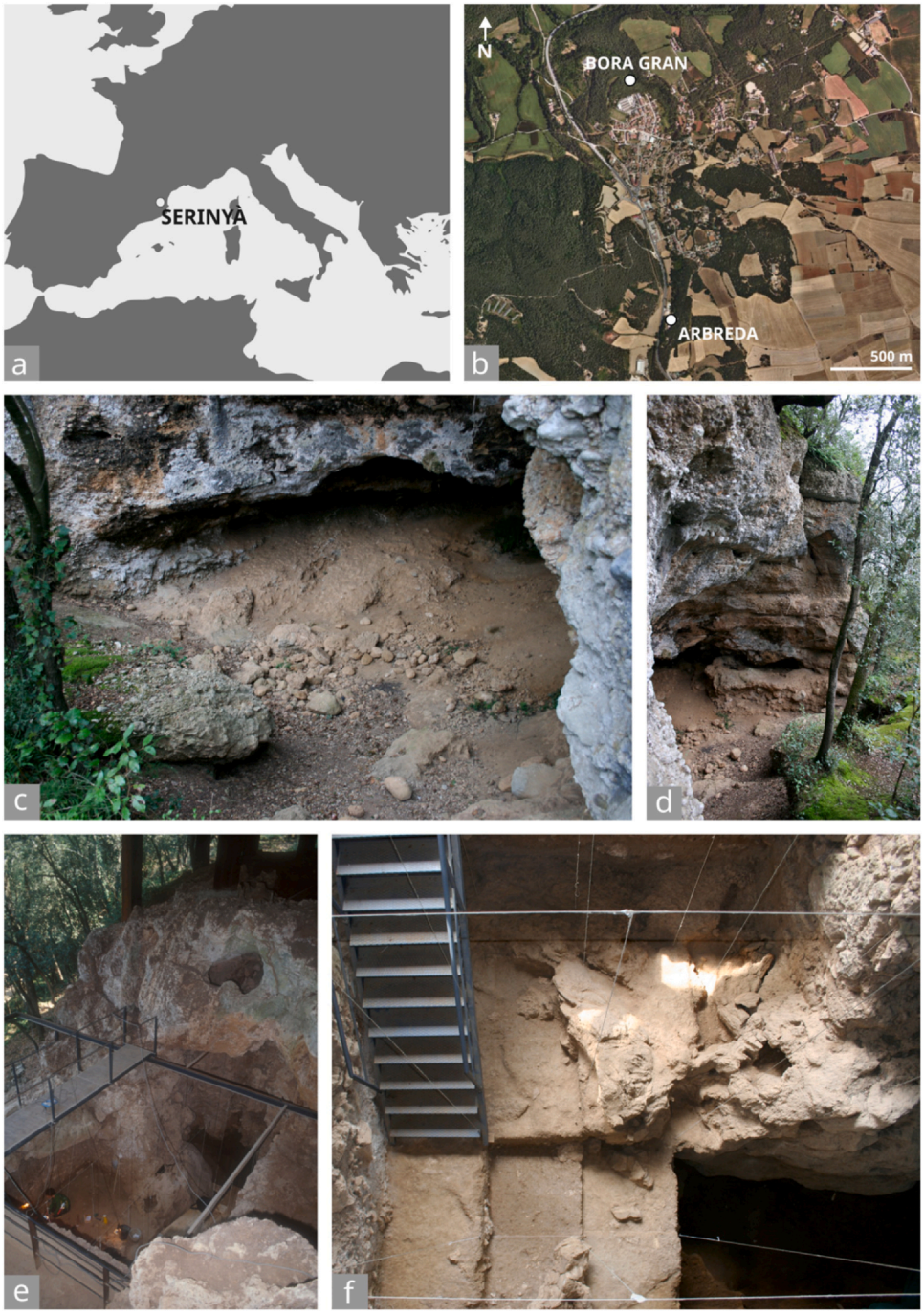

Fig. 1. a) Location of the municipality of Serinyà; b) Emplacement of Bora Gran and Arbreda sites north and south respectively from the town of Serinyà; c) Bora Gran site is a wide rock-shelter carved in conglomerates and open towards east; d) Side view of Bora Gran; e) Excavation of Beta sector from Arbreda cave. The travertine arc is the only remaining part of the roof. Alpha sector lays below it and Gamma Sector behind; f) Zenital view of Beta Sector from Arbreda cave during the excavation of J level, showing at the left the test pit excavated by Josep Maria Corominas (Alpha sector).

are abundant at Bora Gran confirming the advanced phase for the Magdalenian occupation in this site. The radiocarbon dates obtained at Bora Gran (12,830 ± 80 uncal BP and 13,080 ± 90 uncal BP; Nadal, 1998) and at Arbreda (13,700 ± 40 uncal BP) confirm the age of these sequences. The change of settlements at Serinyà by the end of the Upper Palaeolithic, from Arbreda to Bora Gran, is a consequence of the collapse of almost all of the remaining ceilings of the Reclau caves, and in particular of Arbreda.

Both the cultural stratigraphical sequence shown at Arbreda cave and the radiocarbon dates at Bora Gran confirm the continuity in the occupation of the area of Serinyà over the Upper Palaeolithic period. Moreover, the recent identification of a Magdalenian occupation in Arbreda's level A allows us to further underline the continuity of occupation by filling the gap between the Final Solutrean from Arbreda cave and the Upper Magdalenian from Bora Gran.

The materials from Arbreda cave are all curated in the Regional Archaeological Museum of Banyoles, while those of Bora Gran are divided in different museums reflecting the history of the research described above. Alsius' and Corominas' collections are curated in the Regional Archaeological Museum of Banyoles, while Bosoms' collection is curated in the Archaeological Museum of Catalonia located in Girona (MAC-Girona). The Pericot-Maluquer collection is preserved in the

Archaeological Museum of Catalonia (MAC-Barcelona), while the materials unearthed by Harlé are curated in the Musée d'Aquitaine (Bordeaux).

2.1.2. Local environment

During the Upper Palaeolithic, the predominance of steppes and xeric herbs contrasted with the widely spread pine forests of the Middle Palaeolithic still present during the Final Mousterian (Revelles et al., 2022). Expansion episodes of coniferous forests (*Pinus* and *Juniperus*) and meso-thermophilous taxa occurred during phases of milder conditions, such as the Aurignacian occupation of Arbreda (Burjachs and Renault-Miskovsky, 1992; Burjachs, 1993). Pollen record from Banyoles Lake (Pèrez-Obiol and Julià, 1994) and Arbreda cave (López-García et al., 2015) suggest that, around the LGM, the landscape was open and increasingly arid, especially during the Solutrean period. Studies on small mammals indicate a more humid environment in the northeastern Iberian Peninsula than in the rest of Europe, and temperatures were colder than present (Fernández-García et al., 2016). The bird assemblage at Arbreda confirms the occurrence of wetlands, and coniferous and open forest habitats during the Upper Palaeolithic (Lloveras et al., 2022). After the LGM, warming temperature supported the expansion of forest comprising broadleaf deciduous taxa, which progressively took over the coniferous species over the Lateglacial period (Banyoles Lake: Pèrez-Obiol and Julià, 1994, Arbreda cave: Revelles et al., 2022).

2.2. Stable isotope analysis

The stable isotope ratios of carbon ($\delta^{13}C$) in terrestrial herbivores reflect those consumed plants. In temperate and boreal environments, where most plants have the same C_3 photosynthetic pathways, local environmental parameters, such as climate, drive their $\delta^{13}C$ values (e.g. Heaton, 1999). The dominant role of mean annual precipitation over mean annual temperature is reflected by a more positive correlation of plant $\delta^{13}C$ values with higher aridity than with higher temperature (e.g. Diefendorf et al., 2010; Kohn, 2010). The conditions of photosynthesis are also influenced by the vegetation itself. The so-called canopy effect leads to lower $\delta^{13}C$ values in plants that occur under the influence of a dense forest cover due to lower light, higher humidity and an increased contribution of recycled CO_2 derived from plant respiration and/or decomposition over well-mixed atmospheric sources (e.g. Heaton, 1999; Kohn, 2010). Thus, a wetter environment with a higher density of vegetation will lead to lower $\delta^{13}C$ values in plants and their consumers (e.g. Drucker et al., 2008), such as horses and red deer, while a more arid and open environment will be reflected by higher $\delta^{13}C$ values.

The sources and mechanisms of nitrogen intake, together with the conditions of nitrogen cycling in soils, influence the nitrogen isotopic ratios ($\delta^{15}N$) of plants (e.g Högberg, 1997, Craine et al., 2009). Most plants obtain their nitrogen from the soil and the associated mycorrhizae, as is often observed in cold environments where nitrogen is in short supply, which leads them to be depleted in $\delta^{15}N$. This mutualistic relationship also explains the lower $\delta^{15}N$ values in shrubs and trees in comparison with graminoids which are lacking such association (e.g. Michelsen et al., 1996; Högberg, 1997). Increasing precipitation as well as decreasing temperature result in lower $\delta^{15}N$ values in any given type of plant (e.g. Amundson et al., 2003). As a result, browsing herbivores are expected to display lower $\delta^{15}N$ values than grazing ones. Lower $\delta^{15}N$ values in plants and their consumers should also be found in colder and/or wetter conditions.

For large mammals, oxygen isotopic ($\delta^{18}O$) values in the carbonate and phosphate fractions of teeth and bones relate to ingested water (e.g. Longinelli, 1984; Kohn et al., 1996; Kohn and Cerling, 2002). For homoeothermic mammals, there is a constant relationship between the $\delta^{18}O$ values of body water and those of carbonate and phosphate. The body water $\delta^{18}O$ values of terrestrial herbivores in temperate and peri-arctic ecosystems is primarily controlled by the $\delta^{18}O$ values of the drinking water, which are positively correlated with temperature and aridity. Carbonate and phosphate $\delta^{18}O$ values may also reflect respiration and the incorporation of water from food, especially for animals that are non-obligate drinkers (Fricke et al., 1998; Levin et al., 2006). For obligate drinkers, such as horse, or semi-obligate drinkers, such as red deer, the $\delta^{18}O$ values of tooth enamel are expected to reflect those of the local precipitation, controlled by temperature at high and middle latitudes, over the months of the crown formation, even if mineralization pattern and water contribution from plants may lead to the attenuation of the isotopic variability (e.g. Fricke et al., 1998; Hoppe et al., 2004; Stevens et al., 2011).

Isotopic values of carbon and nitrogen are typically measured on bone collagen, which provides a long-term dietary record that averages the last few years the animal's life. Tooth enamel carbonate can also be analysed for stable carbon and oxygen isotopes. Because tooth enamel forms over a limited period without undergoing further remodelling after its completion, it may provide a snapshot of several months from the early phases of an animal's life.

2.3. Dental mesowear and microwear

Dental mesowear and microwear are two proxies commonly used to evaluate the diet of mammals from fossil assemblages. Mesowear is a proxy that evaluates the abrasiveness of the diet in ungulates based on molar cusps relief and shape (Fortelius and Solounias, 2000). Leaf browsers, with a low abrasive diet (leaves from trees and shrubs, herbaceous plants), will have sharp cusps with high relief; while grazers, feeding on very abrasive plants (grasses), will display rounded or blunt cusps with low relief. Mesowear reflects the diet on a long temporal scale of months to years and provides an average of the annual diet (Ackermans et al., 2020).

Microwear is the quantification of the microscopic features (pits and scratches) produced on the tooth occlusal surface by the mastication of food items. The quantification of the microwear features on the enamel is related to the dietary habits in ungulates, with leaf browsers having low numbers of scratches while grazers have high numbers (Solounias and Semprebon, 2002). Microwear corresponds to a short-term signal of days to weeks and thus reflects a more seasonal and local diet than mesowear (Grine, 1986).

3. Material and methods

3.1. Stable isotopes of enamel carbonates

We selected upper and lower third molars of horses from Arbreda (Alpha and Beta sectors) and Bora Gran (collection Bosoms), as well as lower third molars of red deer and two associated second molars for Bora Gran (Table 1). A total of 21 horse molars from the Aurignacian to Solutrean occupations of Arbreda cave were analysed through intra-tooth sequential carbonate analysis, as well as one horse molar could be added from the Magdalenian period of Bora Gran (Table A.1). Red deer teeth are less common at Arbreda, leading to the selection of four third molars equally distributed between level I (Final Mousterian), level F (Gravettian), level E (Gravettian), and level D (Final Gravettian). In contrast, at Bora Gran, 16 third molars and two second molars were available for the Magdalenian period.

For horses, the mineralization of the third molar takes place during the second to fourth year of life and should capture three summer and two winter seasons, as demonstrated by the radiography analyses of mandibles from modern domestic horses (Hoppe et al., 2014). A study of incremental oxygen isotopic analysis of upper teeth from a modern six-year-old horse revealed that only two summer peaks and two winter throughs could be clearly detected in the third molar, corresponding to the third and fourth year of life of the individual (De Winter et al., 2016). The brachydont teeth of the red deer develop over a relatively short period of time. According to radiographic observations by Brown and Chapman (1991), the mineralization of the third molar occurs from

Table 1
Minimum (Min), maximum (Max), mean and standard-deviations (SD) of $\delta^{13}C_{carb}$ and $\delta^{18}O_{carb}$ values per horse and red deer tooth. Numbers in bold indicate isotopic values corresponding to peaks (summer) or troughs (winter) detected from clear sinusoidal patterns in $\delta^{18}O_{carb}$ values. LM3 and UM3 stand for lower third molar and upper third molar, respectively. LM2 stands for lower second molar. R is for the right side, L is for the left side. N: number of analyses.

							$\delta^{13}C_{carb}$ (‰ VPDB)					$\delta^{18}O_{carb}$ (‰ VSMOW)				
Lab ID	**Species**	**Site**	**Excavation**	**Culture**	**Tooth**	**N**	**Min**	**Max**	**Range**	**Mean**	**SD**	**Min**	**Max**	**Range**	**Mean**	**SD**
BOG-HB1	*Equus ferus*	Bora Gran	Coll. Bosoms	Magdalenian	LM3 L	10	-11.1	-10.4	0.7	-10.9	0.3	**23.7**	**25.5**	**1.8**	24.6	0.7
SAR-H8	*Equus ferus*	Arbreda	β, level C	Solutrean	LM3 R	10	-11.2	-10.8	0.4	-11.1	0.1	**25.1**	**26.2**	**1.2**	25.4	0.4
SAR-H9	*Equus ferus*	Arbreda	β, level C	Solutrean	LM3 R	10	-11.6	-11.0	0.6	-11.2	0.2	**25.1**	**26.4**	**1.4**	25.7	0.5
SAR-H10	*Equus ferus*	Arbreda	β, level C	Solutrean	LM3 R	11	-11.9	-11.4	0.5	-11.6	0.2	**24.0**	**25.7**	**1.8**	24.8	0.5
SAR-H11	*Equus ferus*	Arbreda	β, level C	Solutrean	LM3 R	6	-11.4	-11.0	0.4	-11.3	0.2	**24.6**	**25.8**	**1.2**	25.1	0.5
SAR-H15	*Equus ferus*	Arbreda	β, level C	Solutrean	UM3 R	7	-11.3	-11.0	0.4	-11.1	0.1	25.2	**26.4**	1.2	25.9	0.5
SAR-H16	*Equus ferus*	Arbreda	β, level C	Solutrean	UM3 R	10	-12.3	-11.6	0.7	-12.0	0.2	**24.1**	**25.2**	**1.1**	24.5	0.4
SAR-H17	*Equus ferus*	Arbreda	β, level C	Solutrean	UM3 L	10	-11.6	-11.0	0.6	-11.3	0.2	**24.1**	**25.0**	**0.9**	24.5	0.3
SAR-H18	*Equus ferus*	Arbreda	β, level C	Solutrean	UM3 L	8	-11.5	-10.7	0.8	-11.1	0.3	25.1	**26.6**	1.5	26.0	0.5
SAR-H12	*Equus ferus*	Arbreda	β, level D	Final Gravettian	LM3 L	7	-11.8	-11.4	0.4	-11.6	0.1	**24.0**	**25.7**	**1.7**	24.7	0.7
SAR-H19	*Equus ferus*	Arbreda	β, level D	Final Gravettian	UM3 R	10	-11.6	-10.7	0.9	-11.2	0.3	23.7	24.9	1.2	24.6	0.5
SAR-H20	*Equus ferus*	Arbreda	β, level D	Final Gravettian	UM3 L	8	-12.4	-12.1	0.2	-12.3	0.1	24.0	25.3	1.3	24.4	0.4
SAR-H13	*Equus ferus*	Arbreda	β, level E	Gravettian	LM3 R	7	-11.8	-11.3	0.5	-11.5	0.2	24.3	25.7	1.4	25.1	0.5
SAR-H21	*Equus ferus*	Arbreda	β, level E	Gravettian	UM3 L	11	-11.7	-11.0	0.7	-11.5	0.2	**23.2**	**25.8**	**2.7**	24.6	0.9
SAR-H22	*Equus ferus*	Arbreda	β, level E	Gravettian	UM3 L	12	-11.8	-11.2	0.5	-11.4	0.2	**23.0**	**25.3**	**2.3**	23.8	0.8
SAR-H1	*Equus ferus*	Arbreda	α, level 17	Gravettian	LM3 R	6	-11.6	-11.0	0.6	-11.4	0.2	24.3	24.9	0.6	24.7	0.2
SAR-H2	*Equus ferus*	Arbreda	α, level 17	Gravettian	LM3 R	8	-11.6	-11.0	0.6	-11.4	0.2	24.6	26.1	1.5	25.3	0.5
SAR-H3	*Equus ferus*	Arbreda	α, level 18	Gravettian	LM3 L	11	-11.4	-10.5	0.9	-10.9	0.3	**23.9**	**25.7**	**1.8**	25.0	0.6
SAR-H4	*Equus ferus*	Arbreda	α, level 18	Gravettian	LM3 L	9	-12.6	-12.0	0.6	-12.3	0.2	**24.0**	**24.9**	**1.0**	24.5	0.4
SAR-H5	*Equus ferus*	Arbreda	α, level 21–24	Grav./Aur.	LM3 R	11	-11.2	-10.7	0.5	-10.9	0.2	**24.3**	**26.0**	**1.7**	25.0	0.5
SAR-H6	*Equus ferus*	Arbreda	α, level 21–24	Grav./Aur.	LM3 R	11	-12.0	-11.5	0.5	-11.8	0.2	**24.2**	**25.3**	**1.1**	24.8	0.4
SAR-H7	*Equus ferus*	Arbreda	α, level 25	Aurignacian	LM3 R	14	-12.2	-11.6	0.6	-11.9	0.2	**24.3**	**26.1**	**1.8**	25.5	0.5
BOG-R1	*Cervus elaphus*	Bora Gran	Coll. Alsius	Magdalenian	LM3 R	6	-9.8	-8.7	1.2	-9.2	0.5	23.8	25.7	1.9	24.8	0.7
BOG-R2	*Cervus elaphus*	Bora Gran	Coll. Alsius	Magdalenian	LM3 R	5	-10.6	-9.5	1.2	-9.8	0.5	25.4	26.3	0.9	25.9	0.4
BOG-R3	*Cervus elaphus*	Bora Gran	Coll. Alsius	Magdalenian	LM3 R	6	-9.5	-8.5	1.0	-8.8	0.4	**23.4**	25.5	2.1	24.6	0.8
BOG-R4	*Cervus elaphus*	Bora Gran	Coll. Alsius	Magdalenian	LM3 R	7	-11.2	-9.9	1.4	-10.6	0.5	**24.4**	25.7	1.3	25.1	0.4
BOG-R5	*Cervus elaphus*	Bora Gran	Coll. Alsius	Magdalenian	LM3 R	7	-7.8	-6.0	1.8	-6.9	0.6	**24.2**	25.6	1.4	24.7	0.5
BOG-RC2	*Cervus elaphus*	Bora Gran	Coll. Corominas	Magdalenian	LM3 R	4	-9.4	-8.1	1.3	-8.7	0.7	23.2	24.1	0.9	23.5	0.4
BOG-R6	*Cervus elaphus*	Bora Gran	Coll. Alsius	Magdalenian	LM3 R	6	-10.8	-9.5	1.3	-10.1	0.5	23.8	25.7	1.9	24.9	0.8
BOG-RC3	*Cervus elaphus*	Bora Gran	Coll. Corominas	Magdalenian	LM3 R	7	-10.0	-8.5	1.5	-9.2	0.6	**25.2**	27.3	2.2	26.0	0.8
BOG-RC4	*Cervus elaphus*	Bora Gran	Coll. Corominas	Magdalenian	LM3 R	6	-9.5	-8.7	0.9	-9.1	0.3	24.2	25.5	1.3	24.9	0.5
BOG-RC5	*Cervus elaphus*	Bora Gran	Coll. Corominas	Magdalenian	LM3 R	7	-10.5	-9.3	1.3	-9.8	0.4	**23.8**	25.5	1.7	24.4	0.6
BOG-RC1	*Cervus elaphus*	Bora Gran	Coll. Corominas	Magdalenian	LM3 L	6	-9.8	-8.6	1.2	-9.2	0.4	25.4	26.2	0.8	25.8	0.3
BOG-R7	*Cervus elaphus*	Bora Gran	Coll. Alsius	Magdalenian	LM3 L	8	-8.9	-7.9	1.0	-8.3	0.3	**26.0**	27.4	1.3	26.8	0.5
BOG-R8	*Cervus elaphus*	Bora Gran	Coll. Alsius	Magdalenian	LM3 L	7	-9.7	-8.8	0.9	-9.3	0.3	24.7	26.3	1.6	25.4	0.6
BOG-R9	*Cervus elaphus*	Bora Gran	Coll. Alsius	Magdalenian	LM3 L	8	-9.6	-8.7	1.0	-9.2	0.4	24.2	25.9	1.7	25.0	0.6
BOG-R10	*Cervus elaphus*	Bora Gran	Coll. Alsius	Magdalenian	LM3 L	6	-9.7	-8.4	1.3	-9.1	0.6	23.9	24.2	0.3	24.1	0.1
BOG-R11	*Cervus elaphus*	Bora Gran	Coll. Alsius	Magdalenian	LM3 L	5	-10.4	-9.1	1.3	-9.9	0.6	24.7	25.3	0.6	25.1	0.3
SAR-R2	*Cervus elaphus*	Arbreda	β, level D	Final Gravettian	LM3 R	4	-7.8	-6.3	1.5	-6.9	0.7	24.4	25.6	1.2	25.1	0.6
SAR-R4	*Cervus elaphus*	Arbreda	β, level E	Gravettian	LM3 L	4	-9.7	-8.4	1.3	-9.0	0.6	23.9	25.3	1.5	24.4	0.7
SAR-R1	*Cervus elaphus*	Arbreda	β, level F	Gravettian	LM3 L	6	-11.3	-10.3	1.0	-10.6	0.4	**24.1**	26.3	2.2	25.2	0.8
SAR-R3	*Cervus elaphus*	Arbreda	β, level I	Final Mousterian	LM3 R	5	-10.9	-10.7	0.3	-10.8	0.1	**24.4**	25.3	0.9	24.8	0.4
BOG-RC2	*Cervus elaphus*	Bora Gran	Coll. Corominas	Magdalenian	LM2 R	3	-10.0	-9.7	0.2	-9.9	0.1	26.6	27.2	0.5	26.8	0.3
BOG-RC1	*Cervus elaphus*	Bora Gran	Coll. Corominas	Magdalenian	LM2 L	5	-10.4	-9.8	0.6	-10.1	0.2	24.7	25.7	0.9	25.3	0.4

9 to 26 months, covering the whole second year of life, whereas the second molars mineralize from 3 to 9 months, and therefore only include one summer and one winter of the first year of life. Intra-tooth oxygen isotope variation in a modern population of red deer from the Isle of Rum revealed a time sequence from late summer to early spring in the third molars, and from winter/spring to late summer/early autumn in the second molars (Stevens et al., 2011). In other words, the second molars of red deer mainly provide a record of the first summer in life, and the third molars the second winter. Since only the third molar can be securely identified for isolated teeth, both in horse and red deer, we selected the second molars only when they were still embedded in the jawbone.

The uppermost part of the enamel and overlying cementum, when present, was removed and successive bands were drilled with a diamond-coated tip from the occlusal surface (earliest formed enamel) to the enamel root junction (ERJ; latest formed enamel) along the crown axis to collect about 10–15 milligrams (mg) of enamel. Cementum samples were also collected from the horse teeth during the cleaning phase, as well as root dentine for both species (18–20 mg). The pretreatment consisted of adding 1.35 ml of sodium hypochlorite (NaOCl) at a concentration of 2.5 % to the sampled substrate, which was then mixed using a vortex. This step aims to remove the organic fraction and was repeated twice for dentine and cementum samples. The NaOCl solution was removed after 24 hours of constant shaking and samples were rinsed three times with Milli-Q H_2O with in-between centrifuge steps to separate liquid and solid fractions. Next, 1.35 ml of 1 M acetic acid buffered solution (CH_3COOH) was added to remove all secondary carbonates (e.g. Koch et al., 1997). After the solution was homogenised using a vortex, the samples were left for 24 hours on a shaker before rinsing again three times as previously described. The samples were then allowed to dry in an oven at 35 °C for 72 hours. Isotopic analysis was performed on 2.5–3 mg of enamel, dentine, and cementum, using a continuous-flow isotope ratio mass spectrometry (IRMS) in the Senckenberg Centre for Human Evolution and Palaeoenvironment at the University of Tübingen. The sample was reacted with highly concentrated (~99 %) phosphoric acid (H_3PO_4) for 4 h at 70°C. The resulting gaseous CO_2 is then analysed five times over a period of 15 minutes and the isotopic ratios were measured using a MultiFlow-Geo interfaced with Elementar IsoPrime 100 IRMS. Final isotopic ratios are reported per mil (‰) calibrated with international standards (IAEA-603 with $\delta^{13}C$ = +2.46 ‰ and $\delta^{18}O$ = –2.37 ‰ and NBS-18 with $\delta^{13}C$ = –5.01 ‰ and $\delta^{18}O$ = –23.20 ‰), as well as three in-house standards (pure carbonate Laaser Marmor with $\delta^{13}C$ = +1.50 ‰ and $\delta^{18}O$ = –5.20 ‰, pre-treated enamel of elephant with $\delta^{13}C$ = –10.55 ‰ and $\delta^{18}O$ = +1.80 ‰, pre-treated enamel of hippo with $\delta^{13}C$ = –3.80 ‰ and $\delta^{18}O$ = –2.10 ‰). LyticOS software by Elementar was used to carry out multi-point standard isotope calibration by generating a trend line (y = mx + c) that maps measured versus expected isotopic results, which is then used to calibrate sample results. Measurement of uncertainty was monitored using three in-house standards. Overall analytical precision is higher than 0.1 ‰ for $\delta^{13}C$ and better than 0.2 ‰ for $\delta^{18}O$ values.

Carbonate $\delta^{13}C$ and $\delta^{18}O$ values provided by the IRMS measurements are expressed versus VPDB. The $\delta^{18}O_{carb}$ values were also reported in tables in graphs expressed in VSMOW scale following the equation: $\delta^{18}O_{VSMOW} = (1.0309 * \delta^{18}O_{VPDB}) + 30.91$ (Coplen, 1988). We, however, did not convert the $\delta^{18}O_{carb}$ values into $\delta^{18}O$ values of consumed water and ultimately air temperature since this involves several caveats: the isotopic record contained in teeth is dampened compared to the input signal due to discontinuous two step mineralization process and non-linear crown growth (Passey and Cerling, 2002; Blumenthal et al., 2014; Bendrey et al., 2015), and the conversion of carbonate to phosphate $\delta^{18}O$ values through species-specific regressions increases the uncertainty of the estimation of temperature based on regionally-specific relationship (Pryor, 2014; Skrzypek et al., 2016).

To test diagenetic alteration or contamination of the enamel, we monitored the carbonate ($CaCO_3$) content with an expected range of 2.3–5.2 % in weight based on the analysis of modern enamel (Rink and Schwarcz, 1995; Koch et al., 1997; Sponheimer and Lee-Thorp, 1999). Measurements of in-house standards (fossil hippo and elephant enamel from a paleontological site in Chad), which underwent the same pretreatment as the archaeological samples, gave a weight percentage of carbonate from 3.9 % to 6.6 %. Dentine is expected to provide similar or higher carbonate contents compared with the enamel (4.4–8.9 % in dentine *versus* 2.3–5.8 % in enamel of modern cattle; Zazzo et al., 2005, 2006).

3.2. Stable isotopes of bone and dentine collagen

Carbon and nitrogen stable isotope ratios had been previously measured on horse and red deer collagen from the Gravettian levels of Arbreda and Reclau Viver (Wood et al., 2014; Drucker et al., 2021) and the Late Mousterian of Arbreda (Wood et al., 2014) and the associated large bovids (*Bos/Bison* or likely *Bos primigenius*, *Ovibos moschatus*; Rufí et al., 2020a; Drucker et al., 2021). We augmented this corpus of large ungulates with samples from the Magdalenian occupation of Bora Gran (horse n = 3, red deer n = 9, *Bos/Bison* n = 1; collection Alsius, Bosoms and Corominas), the Solutrean levels of Arbreda (Beta sector) and Reclau Viver (level F) (horse n = 8, red deer n = 5, *Bos/Bison* n = 4), the Final Gravettian of Reclau Viver (level D) (red deer, n = 1), the Gravettian of Arbreda (alpha and beta sector) and Mollet III (red deer n = 2) and the Protoaurignacian of Reclau Viver (horse n = 3, red deer n = 5, five red deer, *Bos/Bison* n = 3, level A). Whenever possible, we collected the root from the horse molars selected for carbonate analysis and bone pieces from red deer mandibles to which teeth sampled for enamel were still attached (Table A.4).

After successive cleaning in Milli-Q water and acetone using an ultrasonic bath, the samples were ground to powder manually (grain size < 0.7 mm). To determine bone collagen content, nitrogen elemental analysis was performed using a Vario EL III elemental analyser at the Department of Geosciences, University of Tübingen. Collagen extraction was conducted on samples providing a nitrogen content equal or above 0.4 % in weight (Bocherens et al., 2005) at the Department of Geosciences of the University of Tübingen following an acid-base-acid method based on Longin (1971) with a first step of demineralization in HCl 1 M, a second step in NaOH 0.125 M to remove humic acids and lipids and a final step of gelatinization at pH = 2 at 100°C over 17 hours. After freeze-drying, the samples were collected for elemental and isotopic measurements.

The quality control of the isotopic composition of collagen is based on the content of carbon and nitrogen. A range of atomic C/N ratio ($C:N_{coll}$) between 2.9 and 3.6 was established by DeNiro (1985) for identifying reliable collagen, to which a minimum of 8–13 % in carbon (C_{coll}) content has to be associated (Ambrose, 1990). A more conservative upper limit of 3.5 for $C:N_{coll}$ is recommended for mammals in C_3 environmental contexts (Guiry and Szpak, 2021), as well as a minimum of 30 % in C_{coll} (Van Klinken, 1999) when dealing with low extraction yields (< 1 %; Van der Plicht and Palstra, 2016) and/or low C_{coll} content (< 30 %; van der Plicht and Palstra, 2016), a correlation between isotopic ratios and C:N or C content for a given species may indicate a diagenetic impact (Guiry and Szpak, 2021).

Elemental and isotopic measurements on collagen were conducted in two successively available facility platforms at Tübingen, Germany, and a part was outsourced to London, Ontario, Canada. At the Isotope Geochemistry laboratory of the Department of Geosciences University of Tübingen ca. 1 mg of collagen was collected for elemental analysis (C_{coll}, N_{coll}) and isotopic measurements ($\delta^{13}C_{coll}$, $\delta^{15}N_{coll}$) were performed using an NC2500 CHN-elemental analyzer coupled to a Thermo Quest Delta + XL mass spectrometer. The reproducibility for the content measurement of N and C is 5 %. The $\delta^{13}C$ and $\delta^{15}N$ values are expressed in marine carbonate (V-PDB) and atmospheric nitrogen (AIR),

respectively. The measurements were calibrated using international reference materials USGS24 ($\delta^{13}C$ = –16.00 ‰) and IAEA 305 A ($\delta^{15}N$ = +39.80 ‰). Analytical error, based on within-run replicate measurement of laboratory standards (albumen, modern collagen, USGS 24, IAEA 305 A), was ± 0.1 ‰ for $\delta^{13}C$, ± 0.2 ‰ for $\delta^{15}N$.

At the Geoecology stable isotope platform of the Department of Geoscience, University of Tübingen, 0.4–0.5 mg of collagen was collected for elemental analysis and isotopic analysis. Elemental and isotopic measurements were conducted on a Vario Isotope Cube elemental analyser in conjunction with an IsoPrime 20ision isotope ratio mass spectrometer. The isotopic values were calibrated using the international reference material USGS-40 ($\delta^{13}C$ = –26.39 ‰, $\delta^{15}N$ = –4.5 ‰) and USGS-41 ($\delta^{13}C$ = +37.63, $\delta^{15}N$ = +47.60 ‰) and values were standardised using two in-house standards (modern camel and elk). An analytical error below 0.1 ‰ and 0.2 ‰ (1σ) was determined for $\delta^{13}C$ and $\delta^{15}N$ respectively in all the repeated analyses. The reproducibility error for the amounts of C and N was lower than 1 %.

At the LSIS-AFAR stable isotope facility of the University of Western Ontario, Canada. Collagen samples (0.5 mg) were weighed into tin capsules and combusted in a Costech Elemental Analyzer coupled to a Thermo Delta Plus XL isotope ratio mass spectrometer operated in continuous flow mode, with helium carrier gas. Two standards, USGS-40 and USGS-41 were included for every ten samples and two internal laboratory standards, powdered keratin (MP Biomedicals Inc., Cat No. 90211, Lot No.9966 H) and IAEA-CH-6 ($\delta^{13}C$ = –10.45 ‰) were included to monitor instrument drift and provide a check on accuracy over the course of each analytical session. Isotopic values were provided with a measurement error of ± 0.1 ‰ for $\delta^{13}C$ and ± 0.2 ‰ for $\delta^{15}N$.

To reconstruct the diet carbon isotopic ratios ($\delta^{13}C_{diet}$) from carbonate carbon isotopic ratios ($\delta^{13}C_{carb}$) measured on horse and red deer, it is advisable to apply a trophic discrimination factor adjusted to the metabolic pattern and body mass of the specific species (Tejada-Lara et al., 2018). Ruminant equation and body mass of 220 kg (Cole, 2017) were used for red deer, while non-ruminant equation and body mass of 350 kg (Spiess, 1979) was used for horses. Interestingly, the calculation led to a trophic discrimination factor of +13.6 ‰ in both cases between carbonate and diet. When comparing $\delta^{13}C_{coll}$ with $\delta^{13}C_{carb}$ from the same specimen, an isotopic spacing value of +8.3 ‰ between collagen and carbonate can be applied, following a trophic discrimination factor between collagen and diet of + 5.3 ‰ based on meta-analysis in herbivores (Stephens et al., 2022).

New AMS radiocarbon measurements were performed at Ion Beam Physics Laboratory of ETH Zürich by measuring $^{14}C/^{12}C$ ratios using the MICADAS accelerator mass spectrometry of submitted collagen samples from two horse and seven red deer samples from Bora Gran and Arbreda, which completed the set of direct dating published for the Serinyà caves (Table A.5). These additional dated specimens included two mandibles of red deer from Arbreda for which intra-individual enamel sampling was conducted. The results were calibrated at 2 sigmas based on the IntCal20 curve (Reimer et al., 2020) and using OxCal v. 4.4 interface (Ramsey and Lee, 2013). The taxonomic identification of a few faunal samples was confirmed by submitting collagen subsamples to fingerprinting by Zooarchaeological by Mass Spectrometry (ZooMS) method (Buckley et al., 2009). ZooMS relies on collagen type I amino acid sequence variation detected on produced peptides to differentiate between species. ZooMS MALDI-TOF-MS analysis was conducted at the Department of Geoscience of the University of Tübingen.

3.3. Dental mesowear and microwear

For mesowear, the lower and upper P3 to M3 were sampled for the red deer (n = 87) and only the upper P3 to M3 for the horse (n = 57). For microwear, the lower and upper P3 to M3 were sampled (horse, n = 64), except the upper M3 for the red deer (n = 74) because none was identified as suitable for this study.

Mesowear is a macroscopic quantification of tooth cusps shape and relief. Teeth are classified in 7 categories on a scale from high relief and sharp cusps (category 0) to low relief and blunt cusps (category 6) (Mihlbachler et al., 2011). The mesowear score (MWS) for each sample is obtained from the average of the individual values. Because mesowear is sensitive to ontogenic age, the young individuals with slightly worn teeth and the senile individuals have to be discarded (Fortelius and Solounias, 2000; Rivals et al., 2007).

The method established by Solounias and Semprebon (2002) was employed to quantify the microwear patterns. The occlusal surfaces were cleaned with acetone and then ethanol 96 %. A mold of the surface was created using high-resolution dental silicone (vinylpolysiloxane; Heraeus Provil novo Light Regular set) and the positive cast was produced using transparent epoxy resin. The casts were screened under the stereomicroscope to remove those showing strong taphonomic alteration that erased the dietary microwear pattern (King et al., 1999; Uzunidis et al., 2021; Micó et al., 2024). Microwear is analysed quantitatively at 35x magnification in a standard area of 0.16 mm^2. The number of pits (rounded features) and scratches (elongated features) are quantified in two areas on each specimen and then averaged. Other variables are scored qualitatively: large pits, gouges, hypercoarse scratches, and cross scratches. The scratch width score (SWS) is used to estimate the scratch width for each specimen by categorising the fine scratches (as 0), a mixture of fine and coarse scratches (as 1) and the coarse scratches (as 2). The quantitative data were plotted on a bivariate plot using the R script MicrowearBivaR (Rivals, 2019).

4. Results

4.1. Isotopic data

4.1.1. Preservation of the isotopic signal

The carbonate content provided by the enamel samples were compared with those yielded by dentine for both species and cementum for horses. Horse molars provided a carbonate content ranging from 3.1 % to 5.2 % for enamel, from 5.0 % to 7.0 % for cementum and from 3.7 % to 6.9 % for dentine. Intratooth range in weight percent $CaCO_3$ varied from 0.4 % to 1.4 %. The highest intratooth variability was found in tooth SAR-H10 (Table A.1), but the enamel band with the highest $CaCO_3$ content (4.8% against 3.5-4.1%) also showed stable isotopic ratios comparable to the associated dentine, while a lower $\delta^{18}O_{carb}$ value was expected from the sinusoidal tendency observed for the rest of the crown. This datum was thus considered as contaminated by a possible accidental inclusion of dentine material and was not included in further isotopic interpretation (Table A.1). The same observation, to a lesser extent, was done for SAR-H12 for which the band closest to the root gave a higher weight percent carbonate (4.7 %) than any other part of the crown (4.0–4.2 %; Table A.1). One band with a slightly deviating carbonate content was also excluded from the interpretation for SAR-H17. Finally, the last three bands collected from the crown of SAR-H19 were of dubious reliability due to relatively low carbonate contents (4.0–4.2 % against 4.2–4.8 %) and scattered $\delta^{18}O_{carb}$ values that did not fit the expected sinusoidal pattern (Table A.1).

Carbonate content in red deer molars varied from 2.6 % to 5.3 % in enamel and 4.4–7.7 % in dentine (Table A.2). The intra-tooth range in enamel varied from 0.2 % to 2.4 % in $CaCO_3$. The highest range of variability was found in tooth BOG-RC1 due to a content weight of 5.1 % of $CaCO_3$, while it ranged from 2.6 % to 3.6 % in the rest of the crown. The band with the highest carbonate content provided the lowest enamel $\delta^{13}C_{carb}$ values and was thus discarded from the set of reliable data. As a result of this exclusion, the carbonate content finally varied from 2.6 % to 4.6 % in red deer enamel with an intra-tooth range not exceeding 1.3 % as observed in horse molars.

Among all the tested samples, only two red deer of the Magdalenian of Bora Gran were measured with less than 0.4 % of nitrogen element in the bone and were thus not considered for collagen extraction (Table

A.3). The extraction yields ranged from 1.0 % to 11.6 % for collagen measured for stable isotopes (Table A.3 and A.4) and from 1.2 % to 10.5 % for collagen submitted for radiocarbon dating (Table A.5). A maximum of 47 % and a minimum of 29.8 % in C_{coll} was measured in dated collagen, while a minimum of 22.5 % was detected in collagen considered for stable isotopes (Table A.3 and A.4). Two red deer and one large bovid exhibited collagen with a C_{coll} of less than 30 %. A comparison with the other specimens of the same species and context (Magdalenian at Bora Gran and Protoaurignacian at Reclau Viver) showed that only the red deer specimen from Bora Gran differed from the coeval red deer in $\delta^{13}C_{coll}$ and $\delta^{15}N_{coll}$ values, which was not the case for the specimen from Reclau Viver. We thus decided to remove this sample (BOG-R10bone) from further interpretation of collagen isotopic ratios.

4.1.2. Enamel carbonate isotopic results

The intra-tooth $\delta^{13}C_{carb}$ variability in horses was relatively small with less than 1 ‰ of amplitude between the highest and lowest value per tooth (0.2–0.9 ‰; Table 1). This was illustrated by the flat profiles of the incremental plots reflecting the lack of seasonal contrasts in the dietary signal (Figures A.2). The mean $\delta^{13}C_{carb}$ value per tooth varied from –12.3 ‰ to –10.9 ‰, corresponding to a mean $\delta^{13}C_{diet}$ values from –25.9 ‰ to –24.5 ‰, which was in line with the consumption of C_3 plants in an open environment.

Out of the 22 horse teeth incrementally sampled, only one specimen exhibited a non-sinusoidal $\delta^{18}O_{carb}$ pattern along the tooth crown (SAR-H1, Gravettian, lower molar; Figure A.2–6) and one specimen showed the expected two years record, including two summer and two winter seasons (SAR-H7, Aurignacian, lower molar; Figure A.2–7). The sequential $\delta^{18}O_{carb}$ patterns were inconclusive for three specimens due to a step-like pattern in the upper third molars (SAR-H15, -H18, -H20; Figure A.2–3 and A.2–4). Interestingly, one upper molar right (SAR-H15) and one upper molar left (SAR-H18) were similar in $\delta^{18}O$ values (Figure A.2–3), both in range and trend, which indicated that we likely dealt with the same individual. Two profiles were not as complete as possible because the lowest part of the crown could not be sampled (SAR-H13; Figure A.2–5) or validated (SAR-H19; Figure A.2–4). It was noteworthy that SAR-H13 showed a trend to reflect mainly the summer season, while SAR-H2 (Figure A.2–6) exhibited a U shape $\delta^{18}O_{carb}$ curve corresponding mainly to winter, a limited record likely due to the fragmentary state of the tooth (no ERJ visible and a left crown length of ca. 35 millimetres). Seven specimens provided a sinusoidal $\delta^{18}O$ profile corresponding to a one-year record, including one winter followed by one summer (SAR-H10, -H11, -H16; Figure A.2–2 and A.2–3), or one winter succeeding to one summer (SAR-H17, -H12, -H3, -H4; Figure A.2–3, A.2–4 and A.2–6), both from upper and lower molars. Finally, seven specimens had the record of one year and a half, including one summer with preceding and succeeding winter, including the Magdalenian tooth from Bora Gran and teeth from Solutrean, Gravettian and Gravettian/Aurignacian transition at Arbreda. Upper as well as lower third molars could provide a record including one year and more. Winter and summer seasons could be detected on more than half of the sampled teeth (15 out of 22).

The amplitude of $\delta^{18}O_{carb}$ profiles varied from 0.6 ‰ to 2.7 ‰ of range with most horse teeth exhibiting a range above 1 ‰ between extreme values. In teeth for which winter and summer seasons could be detected (n = 15), the range of values clustered between 0.9 ‰ and 2.7 ‰ for a growth rate of 26–45 mm/year. (Table 1; Figures A.2) The highest winter-summer contrasts were found in specimens from level E at Arbreda (Iberian Middle Gravettian) with a seasonal range of 2.3 ‰ and 2.7 ‰ due to lower winter $\delta^{18}O_{carb}$ values (< +23.5 ‰) than in the other analysed specimens (+23.7 to +25.1 ‰). Apart from this observation, there was no clear trend in the extreme $\delta^{18}O_{carb}$ values related to the stratigraphical position of the specimens. The corresponding winter and summer $\delta^{13}C_{carb}$ values ranged from –12.2 ‰ to –10.6 ‰ and from –12.2 ‰ to –10.8 ‰, respectively, when all individuals are considered. The contrasts in winter and summer values (1.6 and 1.4 ‰ of range, respectively) between individuals were larger than the intra-individual variation (< 1 ‰) and comparable inter-individual differences were observed for each level (e.g. level 18, sector alpha at Arbreda). Interestingly, a trend of higher $\delta^{18}O_{carb}$ values associated with higher $\delta^{13}C_{carb}$ values was observed for both minimum (winter) and maximum values (summer) across the stratigraphic sequence (Fig. 2). Positive co-variation between $\delta^{18}O_{carb}$ and $\delta^{13}C_{carb}$ values may indicate the driving control of aridity. In this case, lower $\delta^{13}C_{carb}$ and $\delta^{18}O_{carb}$ values would result from increasing humidity, such as during the winter seasons experienced by the middle Gravettian horses at Arbreda.

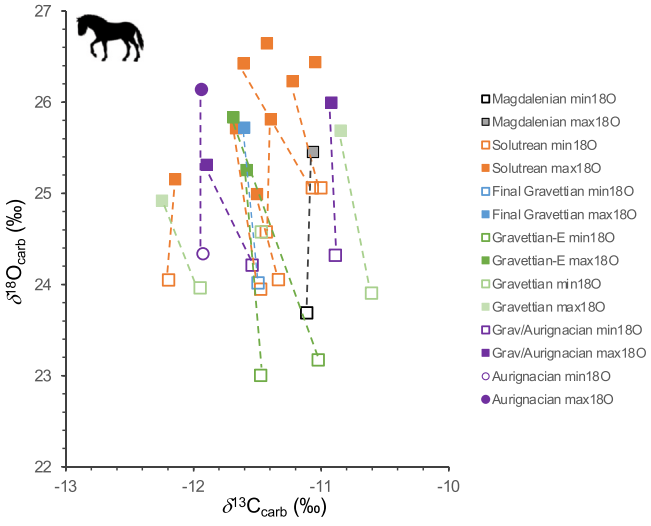

Fig. 2. Minimum and maximum $\delta^{18}O_{carb}$ values for each horse tooth with clear sinusoidal pattern and their corresponding $\delta^{13}C_{carb}$ values. Illustration of an incremental sampling on horse molar on the bottom right part of the graph.

The $\delta^{13}C_{carb}$ of red deer teeth ranged from –11.3 ‰ to –6.0 ‰ in all third molars and from –10.4 ‰ to –8.1 ‰ in the second molars, with an intra-tooth variability ranging from 0.2 to 1.8 ‰ (Table 1). Both $\delta^{13}C_{carb}$ values and intra-tooth ranges were higher than those exhibited by the horse specimens. In red deer for which both second and third molars were sampled, the values clustered between –9.8 ‰ to –8.1 ‰ in third molars, which were higher values than those recorded in the corresponding second molars (from –10.4 ‰ to –9.7 ‰), confirming a substantial contrast between winter (third molars) and summer (second molar) seasons.

Out of 20 third molars, seven showed an inverted U-curve profile (BOG-R5, -R7, -R8, -R9, -RC3, -RC5 and SAR-R1; Figure A.3–2, A.3–4 and A.3–6), two a U-curve profile (BOG-R11, -RC1; Figure A.3–5), and one even a sinusoidal trend in $\delta^{13}C_{carb}$ (BOG-R4; Figure A.3–1). Seven specimens could be considered as displaying a partly recorded inverted U-curve (BOG-R1, -R2, -R6, -R10, -RC2, SAR-R2 and SAR-R4; Figure A.3–1, A.3–2, A.3–3, A.3–5 and A.3–6). The other three specimens (BOG-R3, -RC4 and SAR-R3; Figure A.3–1, A.3–2 and A.3–6) did not show a clear trend in the incremental plots, and their range values were indeed equal to or less than 1 ‰. Mean $\delta^{13}C_{carb}$ values ranged from –10.8 ‰ to –6.9 ‰ ($\delta^{13}C_{diet}$ values from –24.4 ‰ to –20.5 ‰) which supports a large inter-individual variability in the diet and habitat, in addition to a seasonal high contrast found in most of the specimens.

The red deer $\delta^{18}O_{carb}$ values clustered between +23.2 and +27.4 ‰, a range consistent with the one found for the horse specimens (+23.0 ‰ to +26.6 ‰) (Table 1). Seasonal variation in $\delta^{18}O_{carb}$ values could be detected (intra-tooth range from 0.9 ‰ to 2.1 ‰), except for six specimens for which either no clear trend (BOG-R1, -R6, -RC2, -RC4 and SAR-R4; Figure A.3–1, A.3–2, A.3–3 and A.3–6) or no incremental change (BOG-R10; Figure A.3–5) could be observed. Except for BOG-RC4, those teeth nevertheless showed some seasonal signal in

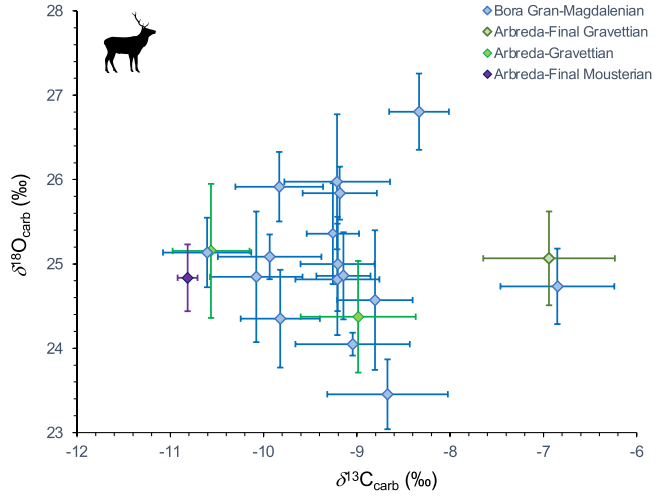

Fig. 3. Means and standard-deviations of $\delta^{13}C_{carb}$ and $\delta^{18}O_{carb}$ values for each sampled third molar of red deer.

their $\delta^{13}C_{carb}$ values. In contrast, BOG-R3 displayed a strong sinusoidal $\delta^{18}O$ trend, while the $\delta^{13}C$ changed only over 1 ‰, suggesting few changes in diet and/or habitat despite contrasted climatic conditions during the formation of the tooth (Figure A.3–1). All the other teeth presented a mirrored pattern in $\delta^{13}C_{carb}$ and $\delta^{18}O_{carb}$ trends. Ten teeth showed a U-curve pattern in $\delta^{18}O_{carb}$ values expected for a molar recording mainly the winter season and a reversed increase in $\delta^{13}C_{carb}$. The left four teeth (BOG-R9, -R11, -RC1 and SAR-R2; Figure A.3–4, A.3–5 and A.3–6) displayed an increase in $\delta^{18}O_{carb}$ values, likely corresponding to summer preceding the expected winter season, with a coeval decrease in $\delta^{13}C_{carb}$ values. The increase in $\delta^{13}C_{carb}$ values, obviously associated with a winter episode, led most of the teeth to reach values above −9 ‰ ($\delta^{13}C_{diet} > -22.6$ ‰) reflecting a xeric environment, or even higher than −7 ‰ ($\delta^{13}C_{diet} > -20.6$ ‰) for BOG-R5 (Figure A.3–2) and SAR-R2 (Figure A.3–6), which can only be reached with the consumption of C_4-like plants. Due to a limited number of pre-LGM samples, it was not possible to examine a chronological trend. However, the same contrasted intra-individual trend and inter-individual values could be found in the pre-LGM samples of Arbreda as illustrated in the Magdalenian of Bora Gran (Fig. 3).

4.1.3. Bone collagen isotopic results

The radiocarbon dates obtained on nine new specimens of horse and red deer were consistent with those already obtained for the same cultural and stratigraphic context (Table A.5; Figures A.4). For Bora Gran, two new dates on red deer fitted in the range of radiocarbon dates obtained previously on deer remains identified as reindeer (*Rangifer tarandus*). The third one is slightly older, fitting the gap between the Magdalenian level A of Arbreda and the Magdalenian occupation of Bora Gran (Figure A.4–1). The dates obtained for level C and E of Arbreda agreed with the date range established for the Solutrean and Gravettian, respectively (Figure A.4–2 and A.4–3). One red deer from Mollet III could be assigned to the same time span as the dated specimens of the Gravettian level F of Arbreda (Figure A.4–3). The last two added samples were from the Mousterian level I of Arbreda and range from 41,750 to 39,410 cal BP, overlapping with the oldest dates of the Protoaurignacian level H. These results confirm the complexity of establishing a clear chronological boundary between these two cultural occupations (Fig. 4).

We considered the collagen results in following the main techno-complexes represented: the Final Mousterian (ca. 54,700–35,400 cal BP), Protoaurignacian (ca. 42,100–35,100 cal BP), Gravettian (33,350–27,150 cal BP), Final Gravettian (ca. 27,350–22,800 cal BP), Solutrean (ca. 23,800–22,500 cal BP) and Magdalenian (16,800–15,000 cal BP) (Table 2).

The $\delta^{13}C_{coll}$ values of horses ranged from –21.6 ‰ to –20.3 ‰ during the Magdalenian (n = 3), which encompassed the degree of variability in the other technocomplexes. Indeed, lower inter-individual differences in $\delta^{13}C_{coll}$ were observed during the Solutrean (–21.1 to –20.4 ‰, n = 8), the Final Gravettian (–20.9 ‰ to –10.6 ‰, n = 5) and the Protoaurignacian (–20.7 to –20.6 ‰, n = 3). A higher diversity in diet and habitat could thus be emphasised for the Magdalenian horses of Bora Gran (Fig. 5).

The horse $\delta^{15}N_{coll}$ values varied from +2.6 ‰ to +7.6 ‰ over the different techno-complexes. The lowest values and variability were found for the Final Gravettian (+2.6 to +3.3 ‰, n = 5), while higher values were observed in other periods, except for one horse of the Protoaurignacian (+3.0 ‰) as well as a larger range (2.6 ‰ to 4.1 ‰ of difference). This could be linked to a higher humidity in the habitat, which was not necessarily reflected by lower $\delta^{18}O_{carb}$ in teeth, since collagen records a longer time span in the ecology of the animal.

The red deer $\delta^{13}C_{coll}$ clustered between –19.6 ‰ and –17.7 ‰, with the highest values above –19.1 ‰ ($\delta^{13}C_{diet} > -24.4$ ‰) found among

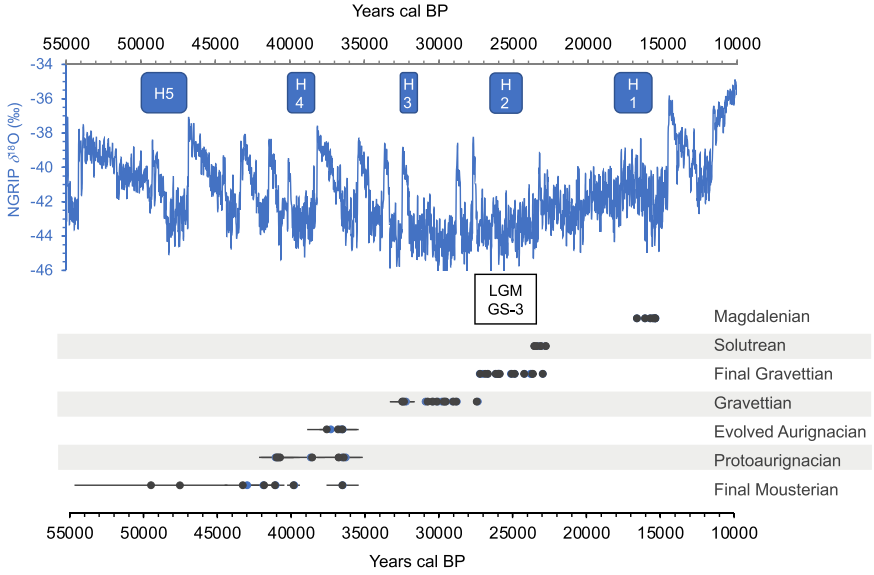

Fig. 4. Calibrated radiocarbon ages reported as median and error bars (2 sigma) for each technocomplexes found at the Serinyà caves in comparison with the NGRIP curve.

Table 2
Minimum (Min), maximum (Max), mean and standard-deviations (SD) of $\delta^{13}C_{coll}$ and $\delta^{15}N_{coll}$ for horse and red deer per technocomplex phases. na stands for not applicable. N: number of samples.

Species	Site	Excavation	Culture	N	$\delta^{13}C_{coll}$ (‰)				$\delta^{15}N_{coll}$ (‰)			
					Min	Max	Range	Mean	SD	Min	Max	Range	Mean	SD
Equus ferus	Bora Gran	Coll. Bosoms	Magdalenian	3	-21.6	-20.3	1.3	-20.8	0.7	3.5	7.6	4.1	5.4	2.1
Equus ferus	Arbreda/Reclau Viver	β, level C/level F	Solutrean	8	-21.1	-20.4	0.7	-20.8	0.2	3.4	7.1	3.7	4.9	1.3
Equus ferus	Arbreda/Reclau Viver	β, level D/level D	Final Gravettian	5	-20.9	-20.6	0.3	-20.8	0.1	2.6	3.3	0.7	3.0	0.3
Equus ferus	Reclau Viver	level A	Protoaurignacian	3	-20.7	-20.6	0.1	-20.7	0.1	3.0	5.6	2.6	4.3	1.3
Equus ferus	Arbreda	β, level I	Final Mousterian	1	-21.2	-21.2	na	na	na	5.0	5.0	na	na	na
Cervus elaphus	Bora Gran	Coll. Alsius, Corominas	Magdalenian	6	-19.6	-17.7	1.9	-18.9	0.7	5.0	7.8	2.8	6.3	1.1
Cervus elaphus	Arbreda	β, level B and C	Solutrean	5	-20.1	-19.5	0.6	-19.8	0.3	3.8	5.7	1.9	5.1	0.8
Cervus elaphus	Arbreda/Reclau Viver	β, level D/level D	Final Gravettian	8	-20.4	-19.5	0.9	-20.1	0.3	4.0	5.7	1.7	4.8	0.5
Cervus elaphus	Arbreda/Mollet III	α level 20, β, level E, F/MIII	Gravettian	6	-20.5	-19.1	1.4	-19.9	0.6	5.0	7.8	2.8	6.5	1.2
Cervus elaphus	Reclau Viver	level A	Protoaurignacian	5	-20.1	-19.7	0.4	-19.9	0.2	4.1	5.4	1.3	4.9	0.5
Cervus elaphus	Arbreda	β, level I	Final Mousterian	5	-20.0	-19.4	0.6	-19.6	0.3	3.1	6.2	3.1	4.9	1.2

the Magdalenian red deer which also exhibited a high variability (2.8 ‰ of range). For each period, the red deer showed higher $\delta^{13}C_{coll}$ values than the coeval horses, without overlapping in most cases. The relatively high $\delta^{13}C_{coll}$ values were driven by foraging in xeric habitat with winter episodes of high ^{13}C-diet detected in the molars that were averaged in the long-term collagen signal.

The red deer $\delta^{15}N_{coll}$ values clustered between +3.1 ‰ and 6.2 ‰ for most of the periods, except during the Gravettian and the Magdalenian (from +5.0 ‰ to +7.8 ‰, n = 6; Table 2, Fig. 5). The ranges of $\delta^{15}N_{coll}$ values overlapped with those of the coeval horses, with the notable exception of the Final Gravettian because of the lower and tightly clustered values of the horses. The Final Gravettian was also the period for which the strongest isotopic niche partitioning among horse, red deer and large bovids was evidenced (Figure A.5). The highest red deer $\delta^{15}N_{coll}$ values (above +6 ‰) were observed in both the Gravettian and the Magdalenian with a difference of up to 2.8 ‰ between the minimum and maximum values. The Magdalenian red deer were also characterised by a high dispersion in the $\delta^{13}C_{coll}$ values (1.9 ‰ of range). These results illustrated an increase in habitat diversity during the warmer phase of the Magdalenian for the red deer, as previously observed for the horse.

4.2. Dental wear results

A total of 144 teeth were examined for the mesowear analysis, 87 identified as red deer and 57 as horse. For microwear, 216 casts were realised, 95 of red deer and 121 of horse. From these casts, 74 of red deer and 64 of horse were suitable for microwear (i.e. 63.9 % of the specimens); the remaining specimens were excluded due to taphonomic alterations that affected the enamel surface.

4.2.1. Mesowear results

The horse, *Equus ferus*, displayed high mesowear scores ranging from 3 to 6 indicating a high abrasive diet corresponding to extant grazing dietary traits (Fig. 6). There was no significant difference among the samples (F test; F = 1.656; df = 15.8; p = 0.2097). The red deer, *Cervus elaphus*, showed a high variability of mesowear scores ranging from 1 to 5 suggesting a low and high proportion of abrasive plants. These mesowear values were overlapping with mesowear scores observed in extant leaf browsers and mixed feeders (Fig. 6). On average, the lowest value, i.e. the stronger browsing signal was found in level F. However, there was no significant difference among the samples (F test; F = 2.126; df = 6.543; p = 0.1868) meaning that there was no significant dietary change among the assemblages analysed from Arbreda and Bora Gran. It is relevant to point out that the mesowear values recorded for the red deer showed a higher variability than that of the horse.

4.2.2. Microwear results

The horse microwear pattern was characterised by high numbers of scratches, very consistent across archaeological levels, and intermediate numbers of pits more variable than the number of scratches (Table 3). These data support the highly abrasive diet previously identified with mesowear. Large pits were observed in all samples with values varying between 21.4 % and 100 % of the individuals. For most of the samples, gouges and hyper-coarse scratches were absent, except in units C, D and E where they were present on various specimens (between 6 % and 40 % of the individuals). Although there were some differences in the qualitative variables, when pits and scratches were considered, the microwear patterns were similar for all the assemblages from Arbreda and Bora Gran as indicated by the overlap of values. These values fell on the 95 % confidence ellipse of extant grazers (Fig. 7). Even if all samples were classified as grazers, the qualitative variables suggest some minor differences in food properties for horse diets among archaeological units. The diet of horses from Arbreda units C, D and E appeared to have been tougher than that of the individuals from the other assemblages.

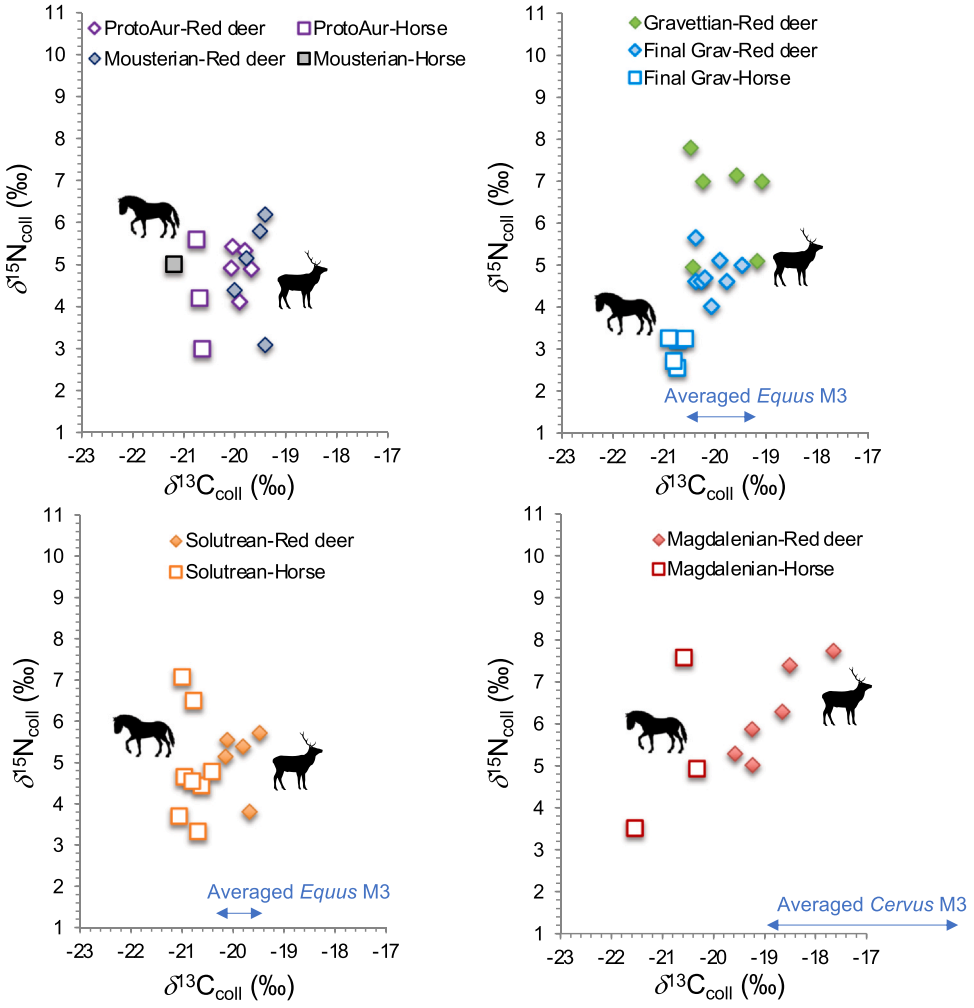

Fig. 5. $\delta^{13}C_{coll}$ and $\delta^{15}N_{coll}$ values of horse and red deer at the Serinyà caves for a) the Late Mousterian (Mousterian) and Protoaurignacian (ProtoAur); b) the Gravettian and Final Gravettian (Final Grav); c) the Solutrean, d) the Magdalenian. Blue double arrows indicate the mean $\delta^{13}C_{carb}$ values of teeth converted in $\delta^{13}C_{coll}$ values.

For the red deer, the number of pits was similar to the horses, but the number of scratches was lower (Table 3). These results confirmed a less abrasive diet than that of the horses, as previously reported using mesowear. The values fell on the ellipse of extant leaf browsers but also in between the browsers and grazers, i.e., in the mixed feeder category (Fig. 7). The stronger browsing signal was found in Arbreda Units F, H and at Bora Gran. The qualitative variables showed strong differences among assemblages. The specimens from Arbreda oldest units H and I did not show large pits, gouges or hypercoarse scratches, while in the other assemblages these features were present in different proportions. These qualitative data indicate a high diversity of plants and plant parts ingested by the red deer. Finally, the microwear patterns in red deer show a higher variability than for the horse, as previously reported from the mesowear analysis.

5. Discussion

All of the $\delta^{13}C$ values from horse and red deer compiled for this study, with $\delta^{13}C_{carb} \geq -12.6$ ‰ and $\delta^{13}C_{coll} \geq -21.6$ ‰, testify to a lack of dense forest cover in their habitat, suggesting the presence of open canopy woodland in the region during pre- and post-LGM periods (e.g. Cerling et al., 1997; Drucker et al., 2008). Relatively high $\delta^{13}C_{coll}$ values in red deer (–20.0 to –19.5 ‰) have also been detected at Teixoneres (Barcelona, Catalonia) around the Middle to Upper Palaeolithic transition (Talamo et al., 2016). Three horse teeth from the Aurignacian level I of Terrasses de la Riera dels Canyars (Gavà, Catalonia) also exhibit high minimum $\delta^{13}C_{carb}$ values (–11.2 to –10.4 ‰) from their incremental analysis (Fernández-García et al., 2023). To our knowledge, our isotopic study of the Serinyà caves is the first extensive one for the Upper Palaeolithic of the Mesomediterranean region of the Iberian Peninsula. Isotopic studies on horse and red deer of the MIS-3 and MIS-2 have been conducted mainly on the Vasco-Cantabrian area in northwestern Iberia, an Eurosiberian region where wetter conditions and more pronounced climatic fluctuations prevailed during the Upper Palaeolithic (e.g. Cascalheira et al., 2021). Several studies on red deer and horses revealed comparable range of $\delta^{13}C_{carb}$ and $\delta^{13}C_{coll}$ values with a minimum equal or above –13 ‰ and –21 ‰, respectively, reflecting also an open landscape (Domingo et al., 2015; Fernández-García et al., 2023). The overlapping values between the two species are explained if they shared the same diet. Alternatively, the expected elevated $\delta^{13}C$ values for a ruminant, such as red deer compared with a non ruminant, such as horse (e.g. Hedges, 2003; Tejada-Lara et al., 2018) may have counterbalanced by the expected higher $\delta^{13}C$ values expected in grazers (here horse) compared with browsers or mixed feeders (here red deer) (e.g. Drucker et al., 2010).

At Serinyà, red deer systematically had higher $\delta^{13}C_{carb}$ and $\delta^{13}C_{coll}$ values compared with those of horse, despite the higher grazing signal for horse than red deer exhibited by the mesowear scores and microwear patterns. Moreover, the red deer of Serinyà show higher $\delta^{13}C_{carb}$ and $\delta^{13}C_{coll}$ values than those found for the equivalent time range in the

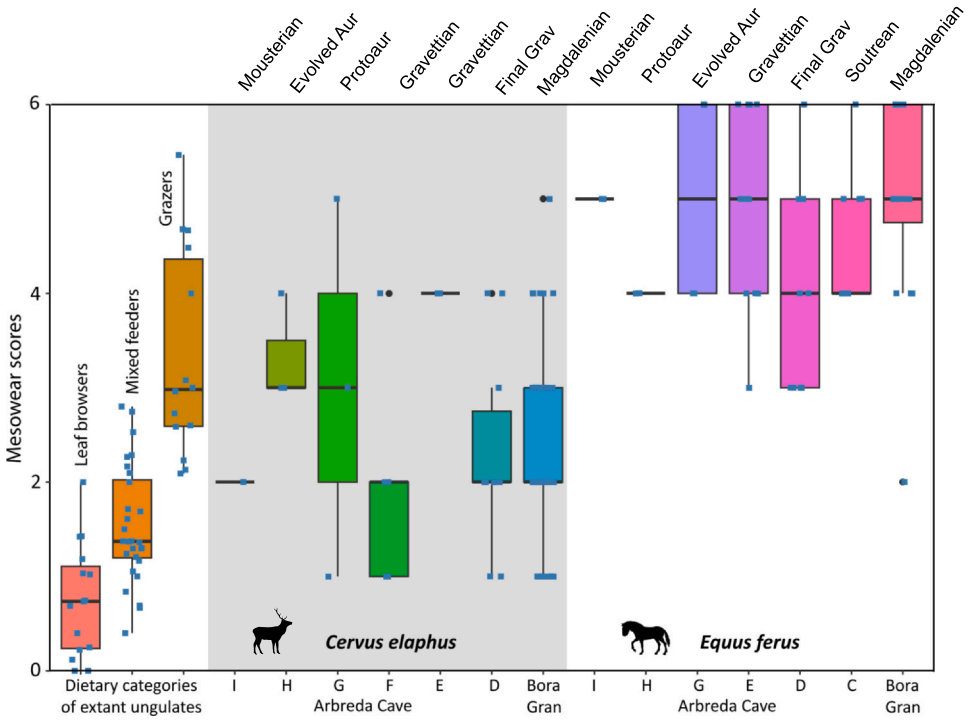

Fig. 6. Boxplot of the mesowear scores (MWS) for the ungulates from Arbreda and Bora Gran compared with the mean values of extant ungulates of different dietary categories (i.e., leaf browsers, mixed feeders, and grazers) based on the reference database from Fortelius and Solounias (2000).

Vasco-Cantabrian region (Jones et al., 2019; Fernández-García et al., 2023). Thus, the red deer $\delta^{13}C_{carb}$ values higher than –9 ‰ were likely driven by foraging in a xeric environment, where the animals could access plants with elevated $\delta^{13}C$ values during the winter season (Cerling and Harris, 1999). This is especially well illustrated with the Magdalenian specimen BOG-R5 at Bora Gran and the Final Gravettian sample SAR-R2 at Arbreda ($\delta^{13}C_{carb}$ values higher than –7 ‰). Thus, consumption of high $\delta^{13}C$ plants during winter was not specific to the most recent period of this study. This seasonality in the diet is found in most of the specimens even when the $\delta^{18}O_{carb}$ values do not vary greatly. It could explain the mesowear scores of the red deer for which no pure browsing signal could be detected. The browsing-based signal of the microwear, especially in the level F (Gravettian) at Arbreda is in line with the season of hunting of red deer from spring to fall during the Iberian middle Gravettian (Level E; Rufí et al., 2019; Figure A.6–1). The lack of specific season in the hunting of red deer during the Final Gravettian (level D; Rufí et al., 2021; Figure A.6–1) may explain a less browsing-oriented microwear pattern. In the modern Mediterranean context, browsing is more intense in summer when herbs become senescent (e.g. Bugalho and Milne, 2003), which is illustrated by the lower $\delta^{13}C_{carb}$ values in the second molars of Bora Gran red deer. The red deer microwear from Bora Gran reveals a strong browsing signal, which suggests a hunting season during spring and summer, but this would need to be confirmed by further zooarchaeological analysis.

Table 3
Summary of the microwear data for the ungulates from Arbreda and Bora Gran.

	Site andunit	Total nb.of molds	Mesowear		Microwear								
Species			N	MWS	N	% preserved	Npit	Nscr	%LP	%G	SWS	%XS	%HC
Cervus elaphus													
	Bora Gran	59	63	2.2	55	93.2	22.8	13.7	100	60	1.3	0	12.7
	Arbreda - D	13	10	2.3	7	53.8	15.2	16.5	71.4	42.9	1	0	14.3
	Arbreda - E	4	2	4	1	25	12	17	100	0	1	0	0
	Arbreda - F	10	5	2	4	40	17.6	14.8	50	50	1	0	25
	Arbreda - G	3	3	3	3	100	8.7	14.8	100	33.3	1.3	0	33.3
	Arbreda - H	3	3	3.3	3	100	10.7	12.3	0	0	0.7	0	0
	Arbreda - I	2	1	2	1	50	12	16	0	0	1	0	0
Equus ferus													
	Bora Gran	23	16	4.9	14	60.9	12.9	22.5	21.4	0	0.9	14.3	0
	Arbreda - B	1	1	4	1	100	9.5	22.5	100	0	1	0	0
	Arbreda - C	37	9	4.6	16	43.2	14.3	22.5	62.5	37.5	1.1	0	6.3
	Arbreda - D	26	13	4	10	38.5	12.4	22.2	60	40	1.2	0	40
	Arbreda - E	20	13	4.9	10	50	15.7	22.7	90	30	1.2	0	30
	Arbreda - G	9	2	5	9	100	14.7	21.8	55.6	0	1.1	0	0
	Arbreda - H	3	1		3	100	15	21.5	66.7	0	1	0	0
	Arbreda - I	2	2	5	1	50	22.5	22	100	0	1	0	0

N = Number of specimens; MWS = Mesowear score; % pres. = Percentage of specimens well preserved for microwear analysis; Npit = Average number of pits; Nscr = Average number of scratches; %LP = Percentage of individuals with large pits; %G = Percentage of individuals with gouges; SWS = Scratch width score; %XS = Percentage of individuals with cross scratches; %HC = Percentage of individuals with hyper-coarse scratches.

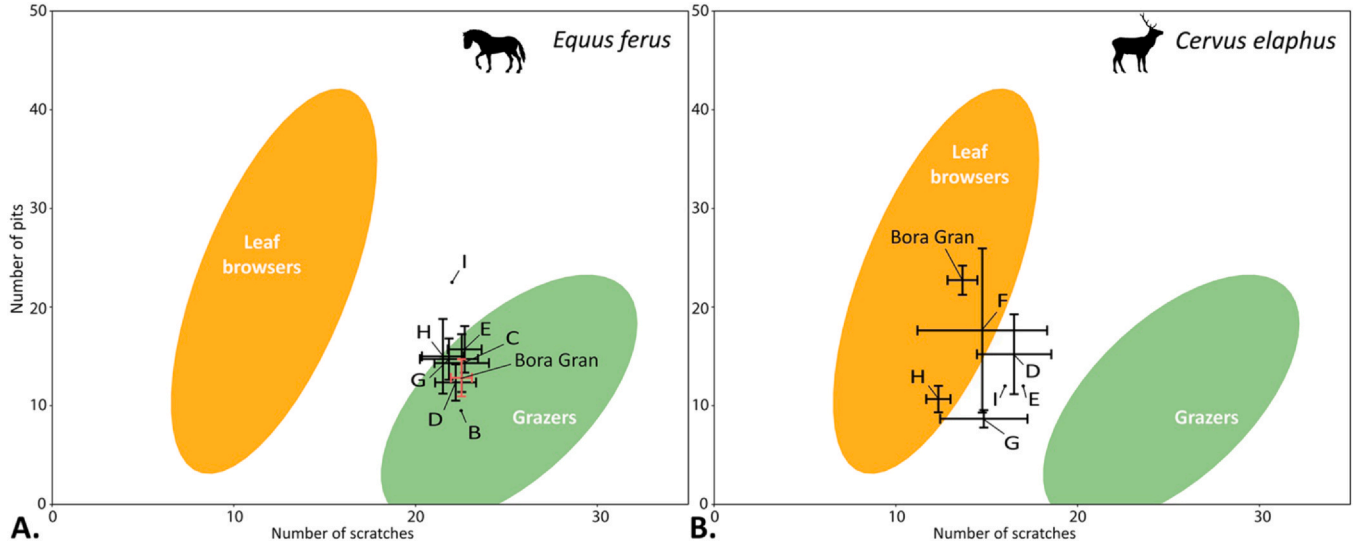

Fig. 7. Bivariate plot of the average numbers of pits and scratches for *Equus ferus* (A) and *Cervus elaphus* (B) from Arbreda and Bora Gran. Error bars correspond to standard error of the mean (± 1 SEM) for each sample. Plain ellipses correspond to the Gaussian confidence ellipses ($p = 0.95$) on the centroid for the extant leaf browsers (LB) and grazers (G) based on the reference database from Solounias and Semprebon (2002).

The horses of Serinyà show a typical grazing signal in the mesowear pattern with a higher variability in the Final Gravettian toward lower scores. The mesowear, in parallel with the relatively lower $\delta^{15}N_{coll}$ values of the horse from level D, suggest a more humid environment. Studies on small mammals reinforce the interpretations of higher humidity in level D than during the earlier phases of the Gravettian at Arbreda (López-García et al., 2015). A high mesowear score, which indicates an intense grazing signal, is found at Bora Gran, but the sole tooth and the few collagen samples analysed for stable isotopes do not indicate any specific dietary signal. Interestingly, the microwear scores of all analysed horses clustered tightly with each other on a pure grazing pattern. Dominant grazing was also observed in horses from the Middle Palaeolithic Unit IIIa of Teixoneres (Unit IIIa) and the Mousterian level J of Arbreda (Sánchez-Hernández et al., 2020). The low intra-tooth variation in $\delta^{13}C_{carb}$ confirms a constant source of forage over the seasons, while the inter-individual contrast in $\delta^{13}C_{carb}$ indicates a change in the habitat conditions from one year to another. Finally, the relative homogeneity in the $\delta^{13}C_{coll}$ among specimens confirms that the inter-year variations were averaged on a long-term basis.

The red deer $\delta^{15}N_{coll}$ values appear to be comparable in their range to those of the horses with the notable exception of the Final Gravettian level D at Arbreda. Higher browsing than grazing should lead to lower $\delta^{15}N$ values in red deer than in horse, based on the difference in $\delta^{15}N$ values between shrubs and grasses (e.g. Michelsen et al., 1996; Högberg et al., 1997). The lower $\delta^{15}N$ values in horses compared with red deer was attributed to a less nutritious forage by Domingo et al. (2015) for the Magdalenian site of La Paloma in Cantabria. Here we attribute the higher $\delta^{15}N$ values of red deer versus horse to a difference between xeric and more humid habitat, a difference even more pronounced during the Final Gravettian at Serinyà. Together with a clear isotopic distinction between horse, red deer and large bovid at that time (Figure A.5), we conclude higher niche partitioning was present during the harsher conditions around the LGM.

6. Conclusions

The capacity of human populations to persist in regions such as the northeastern Iberian Peninsula during the Late Pleistocene was dependent on the terrestrial ecosystem resilience to the climatic instability. Seasonal diet variation recorded in enamel stable isotopes and dental wear in horses and red deer confirm that environmental changes impacted these two ungulates, which played an important role in human subsistence at that time. Interestingly, the relative intra- and inter-individual dietary variability in horses compared with red deer, as expressed by carbon isotopic values and microwear scores, could indicate a more constrained ecological niche. Despite a strong grazing signal over the seasons and years, horses seemed to have favoured a more humid habitat than red deer which foraged on shrubs and xeric plants in a more open and drier environment. The red deer also show a high inter-individual contrast in carbon isotopic values and mesowear scores as well as changing microwear pattern along the stratigraphical sequence, which seems to confirm our hypothesis that the adaptation of the herbivores to a changing environment was possible thanks to their ecological flexibility. However, the persistence of a graze-dominated diet in relatively humid conditions in horses show the importance of the diversity of habitats to buffer the impact of the climatic conditions.

A mosaic landscape may have allowed large herbivores to find forage and habitat compensating for the change in the climatic conditions, a scenario that has been suggested for the Vasco-Cantabrian region (Jones et al., 2020; Fernández-García et al., 2023). The high ecological flexibility of the red deer allowed it to occupy contrasted niche not only in comparison with the horse but also with deer from other regions of the Iberian Peninsula. On the other hand, access to relatively wet local patches seems to have played a key role for horses in buffering the impact of the climatic conditions. Altogether, the results on red deer and horse bring a more nuanced view on the functioning of the northeastern Iberian Peninsula as a refuge zone.

CRediT authorship contribution statement

Dorothée G. Drucker: Conceptualization, Data curation, Funding acquisition, Investigation, Methodology, Project administration, Supervision, Visualization, Writing – original draft, Writing – review & editing. **Florent Rivals:** Conceptualization, Formal analysis, Investigation, Methodology, Visualization, Writing – original draft, Writing – review & editing. **Jordi Nadal:** Conceptualization, Resources, Writing – review & editing. **Isaac Rufí:** Resources, Visualization, Writing – original draft. **Joaquim Soler:** Conceptualization, Data curation, Resources, Visualization, Writing – original draft, Writing – review & editing. **Narcís Soler:** Resources, Writing – original draft. **Julià Maroto:** Conceptualization, Data curation, Resources, Visualization, Writing – review & editing.

Data availability

Datasets related to this article can be found at https://doi.org/10.5281/zenodo.11108332 (Drucker, 2024) and https://doi.org/10.5281/zenodo.10961000 (Rivals, 2024), an open-source online data repository hosted at Zenodo.

Declaration of Competing Interest

The authors declare that they have no known competing financial interests or personal relationships that could have appeared to influence the work reported in this paper.

Acknowledgements

Thanks are due to Andrea Ferrer Welsch (Regional Archaeological Museum Banyoles), Lluís Lloveras Roca (University of Barcelona), and Ramon Buxó Capdevila (Museu d'Arqueologia de Catalunya-Girona) for their support during the selection of the material of study. We are grateful to Keith Hobson (Western University Ontario, Canada), Bernd Steinhilber, Sabine Faiz, Valentina García-Huidobro, Valentina García-Huidobro, íNolan Ferar, Sanah Shaikh, Ruth Rey, Chrysoula Tsimopoulou (Department of Geoscience, University of Tübingen), and Peter Tung (Senckenberg HEP, University of Tübingen) for their technical and scientific support. We also thank Irka Hajdas (ETH, Zürich) and Samantha Brown (Department of Geoscience, University of Tübingen) for their contribution to additional data, Maciej Krajcarz (Institute of Geological Sciences, Polish Academy of Sciences) for commenting the manuscript, and Emily Milton (Department of Anthropology, Michigan State University) for editing the English language.

This work was supported by the DFG project EcoRef DR945/6-1 "Ecological response of large herbivores to the late Quaternary Climatic Changes in Northeast Iberian Peninsula Refugium" Project number 427557110. DD benefited from the financial support of the Leakey Foundation for a previous pilot study. Travels to access the collections for FR, IR and JM in Girona and Banyoles were supported by grants PID2022-138590NB-C41 and PID2022-138590NB-C44 (doi MCIN/AEI/10.13039/501100011033) and by "ERDF A way of making Europe".

Appendix A. Zooarcheological information on horse and red deer in northeastern Iberian Peninsula during the Late Pleistocene

Table A1
Detailed isotopic results ($\delta^{13}C_{carb}$ and $\delta^{18}O_{carb}$) for horse teeth with incremental sampling. Underlined numbers correspond to outlier data. Brackets are added around isotopic values that are not considered for further interpretation. R stands for the right side, L is for the left side.

Site	Tooth	Inventory	Tissue	Lab ID	Crown height (mm)	Distance from the ERJ (mm)	Distance from the lowest crown part (mm)	CaCO3 (%)	$\delta^{13}C_{carb}$ (‰ VPDB)	$\delta^{18}O_{carb}$ (‰ VPDB)	$\delta^{18}O_{carb}$ (‰ VSMOW)
Bora Gran	Lower M3 L	Bosoms #6113	enamel	BOG-HB1a	58.0	54.7		4.0	-11.1	-5.3	25.4
			enamel	BOG-HB1b		50.6		3.6	-11.1	-5.7	25.0
			enamel	BOG-HB1c		45.7		3.8	-11.1	-7.0	23.7
			enamel	BOG-HB1d		40.7		3.9	-10.9	-6.0	24.8
			enamel	BOG-HB1e		33.4		4.1	-10.4	-5.5	25.2
			enamel	BOG-HB1f		28.1		3.5	-10.8	-5.9	24.9
			enamel	BOG-HB1g		22.2		3.7	-10.9	-5.5	25.3
			enamel	BOG-HB1h		17.2		3.8	-10.7	-6.6	24.1
			enamel	BOG-HB1i		11.7		3.6	-10.9	-6.9	23.8
			enamel	BOG-HB1j		8.0		3.9	-10.5	-6.7	24.0
			cementum	BOG-HB1CEM		-		5.0	-9.8	-7.2	23.5
Arbreda	Lower M3 R	E5 EE26 #418	enamel	SAR-H8a	50.1		46.7	4.7	-11.2	-5.4	25.4
Beta sector Level C			enamel	SAR-H8b			43.2	4.6	-10.8	-5.4	25.3
			enamel	SAR-H8c			38.8	4.5	-11.0	-5.3	25.5
			enamel	SAR-H8d			33.1	4.2	-11.0	-5.7	25.1
			enamel	SAR-H8e			28.6	3.9	-11.2	-5.4	25.3
			enamel	SAR-H8f			23.5	4.2	-11.2	-4.5	26.2
			enamel	SAR-H8g			18.4	4.2	-11.2	-5.0	25.8
			enamel	SAR-H8h			13.4	4.3	-11.1	-5.6	25.1
			enamel	SAR-H8i			10.0	4.2	-11.2	-5.6	25.2
			enamel	SAR-H8j			5.1	3.9	-10.9	-5.4	25.4
			cementum	SAR-H8CEM			-	5.6	-10.6	-4.7	26.1
Arbreda	Lower M3 R	C4 DC10 #362	enamel	SAR-H9a	49.8	47.87		3.8	-11.1	-5.2	25.6
Beta sector Level C			enamel	SAR-H9b		43.96		3.8	-11.1	-5.7	25.1
			enamel	SAR-H9c		39.87		4.0	-11.0	-5.1	25.6
			enamel	SAR-H9d		35.61		3.7	-11.1	-5.3	25.5
			enamel	SAR-H9e		31.19		4.0	-11.4	-4.7	26.1
			enamel	SAR-H9f		27.21		4.1	-11.6	-4.4	26.4
			enamel	SAR-H9g		23.09		3.9	-11.4	-5.5	25.3
			enamel	SAR-H9h		18.53		3.9	-11.3	-5.6	25.2
			enamel	SAR-H9i		14.26		3.8	-11.3	-4.8	26.0
			enamel	SAR-H9j		10.68		3.8	-11.1	-4.6	26.2
			cementum	SAR-H9CEM		-		5.9	-11.2	-4.8	26.0
Arbreda	Lower M3 R	E5 EE27 #500	enamel	SAR-H10a	53.0	49.8		3.4	-11.4	-5.4	25.3

(*continued on next page*)

Table A1 (*continued*)

Site	Tooth	Inventory	Tissue	Lab ID	Crown height (mm)	Distance from the ERJ (mm)	Distance from the lowest crown part (mm)	CaCO3 (%)	$\delta^{13}C_{carb}$ (‰ VPDB)	$\delta^{18}O_{carb}$ (‰ VPDB)	$\delta^{18}O_{carb}$ (‰ VSMOW)
Beta sector			enamel	SAR-H10b		46.4		3.7	-11.4	-6.2	24.5
Level C			enamel	SAR-H10c		43.2		3.8	-11.4	-6.5	24.3
			enamel	SAR-H10d		38.3		4.0	-11.5	-6.8	23.9
			enamel	SAR-H10e		33.6		4.1	-11.6	-6.3	24.4
			enamel	SAR-H10f		29.5		3.8	-11.8	-6.1	24.6
			enamel	SAR-H10g		24.0		3.9	-11.9	-5.5	25.2
			enamel	SAR-H10h		21.2		3.5	-11.7	-5.9	24.8
			enamel	SAR-H10i		17.9		3.7	-11.7	-5.4	25.4
			enamel	SAR-H10j		13.9		3.5	-11.7	-5.0	25.7
			enamel	SAR-H10k		10.4		3.7	-11.6	-5.7	25.0
			enamel	SAR-H10l		6.9		4.8	(-11.5)	(-5.0)	(25.7)
			cementum	SAR-H10CEM		-		5.3	-11.5	-5.4	25.4
Arbreda	Lower M3 R	B2 BB13 #250	enamel	SAR-H11a	27.6	25.2		3.5	-11.3	-6.1	24.7
Beta sector			enamel	SAR-H11b		22.0		3.4	-11.4	-6.1	24.6
Level C			enamel	SAR-H11c		18.7		3.8	-11.2	-6.0	24.7
			enamel	SAR-H11d		15.0		3.9	-11.0	-5.7	25.1
			enamel	SAR-H11e		10.9		4.3	-11.2	-5.1	25.7
			enamel	SAR-H11f		6.5		nd	nd	nd	nd
			enamel	SAR-H11g		2.9		4.8	-11.4	-5.0	25.8
			cementum	SAR-H11CEM		-		6.5	-9.4	-5.1	25.6
			dentine	SAR-H11DEN		-		6.7	-10.8	-5.0	25.8
Arbreda	Upper M3 R	E4 DE16 #219	enamel	SAR-H15a	42.2	39.9		4.7	-11.1	-4.4	26.3
Beta sector			enamel	SAR-H15b		34.7		4.6	-10.9	-4.4	26.4
Level C			enamel	SAR-H15c		30.6		4.7	-11.0	-4.3	26.4
			enamel	SAR-H15d		24.8		4.1	-11.2	-4.8	26.0
			enamel	SAR-H15e		19.4		4.2	-11.1	-5.3	25.5
			enamel	SAR-H15f		13.3		4.1	-11.1	-5.0	25.7
			enamel	SAR-H15g		7.1		4.6	-11.3	-5.5	25.2
			cementum	SAR-H15CEM		-		6.6	-10.2	-6.3	24.4
			dentine	SAR-H15DEN		-		5.5	-10.2	-7.1	23.6
Arbreda	Upper M3 R	C3 CC11 #553	enamel	SAR-H16a	63.5		55.2	4.7	-11.7	-6.0	24.8
Beta sector			enamel	SAR-H16b			50.9	4.6	-11.8	-6.6	24.1
Level C			enamel	SAR-H16c			45.4	4.6	-11.6	-6.3	24.4
			enamel	SAR-H16d			39.1	4.6	-11.9	-6.6	24.1
			enamel	SAR-H16e			34.2	4.5	-12.2	-6.7	24.0
			enamel	SAR-H16f			29.2	4.8	-12.1	-6.5	24.3
			enamel	SAR-H16g			23.4	5.0	-12.3	-6.2	24.6
			enamel	SAR-H16h			18.4	4.6	-12.1	-5.6	25.2
			enamel	SAR-H16i			12.5	4.8	-12.2	-5.9	24.8
			enamel	SAR-H16j			7.9	4.9	-12.1	-5.9	24.8
			cementum	SAR-H16CEM			-	5.2	-11.2	-6.7	24.4
			dentine	SAR-H16DEN			-	6.1	-11.6	-7.9	22.7
Arbreda	Upper M3 L	C3 CC11 #467	enamel	SAR-H17a	63.4		54.8	4.8	(-11.3)	(-5.9)	(24.9)
Beta sector			enamel	SAR-H17b			50.1	4.6	-11.1	-6.2	24.5
Level C			enamel	SAR-H17c			45.4	4.7	-11.1	-6.2	24.6
			enamel	SAR-H17d			40.4	4.7	-11.4	-6.1	24.6
			enamel	SAR-H17e			34.7	4.4	-11.3	-5.9	24.8
			enamel	SAR-H17f			30.0	4.4	-11.5	-6.5	24.2
			enamel	SAR-H17g			23.3	4.2	-11.3	-6.7	24.1
			enamel	SAR-H17h			18.0	4.6	-11.4	-6.6	24.1
			enamel	SAR-H17i			12.4	4.1	-11.6	-6.2	24.5
			enamel	SAR-H17j			8.0	4.6	-11.5	-5.7	25.0
			enamel	SAR-H17k			3.3	4.3	-11.0	-6.5	24.2
			cementum	SAR-H17CEM			-	5.6	-10.5	-5.8	25.0
			dentine	SAR-H17DEN			-	5.8	-11.3	-7.6	23.1
Arbreda	Upper M3 L	D3 CD11 #350	enamel	SAR-H18a	41.3	38.1		4.7	-11.4	-4.5	26.3
Beta sector			enamel	SAR-H18b		33.7		4.6	-11.4	-4.1	26.6
Level C			enamel	SAR-H18c		29.6		4.4	-11.3	-4.7	26.1
			enamel	SAR-H18d		25.7		4.5	-11.1	-4.8	25.9
			enamel	SAR-H18e		20.5		4.3	-11.2	-5.0	25.8
			enamel	SAR-H18f		15.1		4.0	-11.2	-4.6	26.2
			enamel	SAR-H18g		10.6		4.3	-10.6	-5.0	25.8
			enamel	SAR-H18h		5.8		5.2	-10.9	-5.6	25.1
			cementum	SAR-H18CEM		-		6.1	-10.3	-6.6	24.1
			dentine	SAR-H18DEN		-		6.9	-11.0	-7.5	23.2

(*continued on next page*)

Table A1 (*continued*)

Site	Tooth	Inventory	Tissue	Lab ID	Crown height (mm)	Distance from the ERJ (mm)	Distance from the lowest crown part (mm)	CaCO3 (%)	$\delta^{13}C_{carb}$ (‰ VPDB)	$\delta^{18}O_{carb}$ (‰ VPDB)	$\delta^{18}O_{carb}$ (‰ VSMOW)
Arbreda	Lower M3 L	E5 EE25 #331	enamel	SAR-H12a	34.5	32.3		4.0	-11.5	-5.5	25.2
Beta sector			enamel	SAR-H12b		29.0		4.0	-11.5	-5.5	25.3
Level D			enamel	SAR-H12c		24.8		4.2	-11.6	-5.0	25.7
			enamel	SAR-H12d		20.3		4.0	-11.5	-5.9	24.8
			enamel	SAR-H12e		14.6		4.2	-11.5	-6.7	24.0
			enamel	SAR-H12f		11.2		4.1	-11.8	-6.7	24.0
			enamel	SAR-H12g		7.1		4.0	-11.4	-6.6	24.1
			enamel	SAR-H12h		4.0		4.7	(-11.4)	(-6.5)	(24.2)
			cementum	SAR-H12CEM		-		6.4	-11.7	-5.0	25.7
Arbreda	Upper M3 R	B5 EB8 #74	enamel	SAR-H19a	69.3	65.1		4.3	-11.3	-6.2	24.5
Beta sector			enamel	SAR-H19b		61.3		4.6	-11.5	-6.2	24.5
Level D			enamel	SAR-H19c		56.1		4.7	-11.3	-6.3	24.4
			enamel	SAR-H19d		51.3		4.6	-11.5	-6.3	24.4
			enamel	SAR-H19e		47.4		4.4	-11.5	-6.0	24.7
			enamel	SAR-H19f		42.6		4.8	-11.6	-5.9	24.8
			enamel	SAR-H19g		37.2		4.7	-11.2	-5.8	24.9
			enamel	SAR-H19h		33.3		4.5	-11.0	-6.8	23.9
			enamel	SAR-H19i		27.8		4.5	-10.7	-6.2	24.6
			enamel	SAR-H19j		23.1		4.2	-10.8	-7.0	23.7
			enamel	SAR-H19k		17.8		4.0	(-11.1)	(-5.5)	(25.2)
			enamel	SAR-H19l		13.1		4.0	(-10.7)	(-6.5)	(24.2)
			enamel	SAR-H19m		8.3		4.2	(-10.8)	(-5.4)	(25.3)
			cementum	SAR-H19CEM		-		6.2	-10.5	-6.7	24.0
			dentine	SAR-H19DEN		-		3.7	-11.5	-8.1	22.6
Arbreda	Upper M3 L	E5 EE28 #504	enamel	SAR-H20a	57.8		56.2	4.9	-12.2	-6.7	24.0
Beta sector			enamel	SAR-H20b			50.3	4.7	-12.4	-5.9	24.8
Level D			enamel	SAR-H20c			45.4	4.9	-12.3	-6.7	24.0
			enamel	SAR-H20d			40.7	4.8	-12.1	-5.8	24.9
			enamel	SAR-H20e			35.4	4.3	-12.3	-6.2	24.5
			enamel	SAR-H20f			30.8	4.8	-12.4	-5.6	25.1
			enamel	SAR-H20g			26.2	4.6	-12.3	-5.5	25.3
			enamel	SAR-H20h			22.3	4.8	-12.2	-6.0	24.7
			cementum	SAR-H20CEM			-	5.6	-12.0	-8.0	22.6
			dentine	SAR-H20DEN			-	5.4	-12.5	-8.2	22.5
Arbreda	Lower M3 R	E5 EE29 #542	enamel	SAR-H13a	54.7	52.9		4.0	-11.3	-6.4	24.3
Beta sector			enamel	SAR-H13b		49.7		4.0	-11.3	-6.1	24.6
Level E			enamel	SAR-H13c		45.1		4.1	-11.5	-5.9	24.8
			enamel	SAR-H13d		41.7		3.8	-11.6	-5.5	25.2
			enamel	SAR-H13e		37.8		4.2	-11.5	-5.3	25.4
			enamel	SAR-H13f		33.8		4.2	-11.6	-5.1	25.6
			enamel	SAR-H13g		29.2		3.4	-11.8	-5.0	25.7
			cementum	SAR-H13CEM		-		6.5	-11.3	-5.0	25.7
Arbreda	Upper M3 L	E0 OE77 #2524	enamel	SAR-H21a	66.5	61.4		4.6	-11.2	-5.5	25.3
Beta sector			enamel	SAR-H21b		56.2		4.7	-11.3	-6.1	24.7
Level E			enamel	SAR-H21c		50.7		4.9	-11.4	-5.7	25.1
			enamel	SAR-H21d		44.2		4.3	-11.4	-6.5	24.2
			enamel	SAR-H21e		37.6		4.3	-11.7	-5.2	25.6
			enamel	SAR-H21f		32.4		4.6	-11.7	-4.9	25.8
			enamel	SAR-H21g		26.9		4.7	-11.6	-5.3	25.4
			enamel	SAR-H21h		21.6		4.6	-11.4	-7.2	23.5
			enamel	SAR-H21i		16.3		4.8	-11.5	-6.9	23.8
			enamel	SAR-H21j		10.7		4.7	-11.7	-6.8	23.9
			enamel	SAR-H21k		5.7		4.3	-11.0	-7.5	23.2
			cementum	SAR-H21CEM		-		6.8	-10.1	-7.4	23.3
			dentine	SAR-H21DEN		-		5.9	-10.3	-8.5	22.2
Arbreda	Upper M3 L	E5 EE34 #678	enamel	SAR-H22a	70.9	66.4		4.9	-11.4	-6.4	24.3
Beta sector			enamel	SAR-H22b		62.5		4.5	-11.4	-7.6	23.1
Level E			enamel	SAR-H22c		56.0		4.7	-11.5	-7.2	23.4
			enamel	SAR-H22d		50.4		4.5	-11.5	-7.7	23.0
			enamel	SAR-H22e		44.3		4.6	-11.4	-7.5	23.2
			enamel	SAR-H22f		39.9		4.6	-11.6	-5.5	25.2
			enamel	SAR-H22g		34.2		4.8	-11.4	-5.6	25.1
			enamel	SAR-H22h		28.6		4.6	-11.2	-6.5	24.2
			enamel	SAR-H22i		22.8		4.6	-11.2	-7.3	23.4

(*continued on next page*)

Table A1 (*continued*)

Site	Tooth	Inventory	Tissue	Lab ID	Crown height (mm)	Distance from the ERJ (mm)	Distance from the lowest crown part (mm)	CaCO3 (%)	$\delta^{13}C_{carb}$ (‰ VPDB)	$\delta^{18}O_{carb}$ (‰ VPDB)	$\delta^{18}O_{carb}$ (‰ VSMOW)
			enamel	SAR-H22j		17.0		4.8	-11.3	-7.5	23.2
			enamel	SAR-H22k		11.5		4.6	-11.7	-7.1	23.6
			enamel	SAR-H22l		6.9		4.5	-11.5	-6.9	23.8
			cementum	SAR-H22CEM		-		6.0	-10.7	-7.9	22.8
			dentine	SAR-H22DEN		-		4.4	-11.2	-8.6	22.0
Arbreda	Lower M3 R	A1 R-55.003	enamel	SAR-H1a	45.4		32.0	5.0	-11.0	-5.9	24.9
Alpha sector			enamel	SAR-H1b			27.0	4.8	-11.4	-6.2	24.6
Level 17			enamel	SAR-H1c			21.8	5.0	-11.5	-6.0	24.7
			enamel	SAR-H1d			16.6	4.3	-11.6	-6.4	24.3
			enamel	SAR-H1e			12.4	4.1	-11.5	-5.9	24.8
			enamel	SAR-H1f			7.7	4.4	-11.3	-6.0	24.7
			cementum	SAR-H1CEM			-	6.9	-9.0	-5.2	25.5
Arbreda	Lower M3 R	O2 R-56.900	enamel	SAR-H2a	34.8		31.6	4.5	-11.4	-4.9	25.8
Alpha sector			enamel	SAR-H2b			28.0	4.2	-11.6	-5.3	25.4
Level 17			enamel	SAR-H2c			23.6	4.3	-11.6	-5.5	25.3
			enamel	SAR-H2d			20.3	4.3	-11.5	-5.7	25.1
			enamel	SAR-H2e			17.8	3.9	-11.5	-6.1	24.6
			enamel	SAR-H2f			14.8	4.1	-11.3	-6.0	24.7
			enamel	SAR-H2g			10.0	3.8	-11.0	-5.6	25.1
			enamel	SAR-H2h			4.5	4.3	-11.2	-4.7	26.1
			cementum	SAR-H2CEM			-	6.8	-8.7	-4.5	26.3
Arbreda	Lower M3 L	B2 R-56.421	enamel	SAR-H3a	49.8		47.3	4.3	-10.9	-5.4	25.3
Alpha sector			enamel	SAR-H3b			43.0	4.4	-11.1	-5.6	25.1
Level 18			enamel	SAR-H3c			39.6	3.9	-10.5	-5.1	25.7
			enamel	SAR-H3d			34.9	4.0	-11.2	-5.2	25.5
			enamel	SAR-H3e			29.9	4.1	-11.4	-5.4	25.4
			enamel	SAR-H3f			25.0	4.2	-10.8	-5.1	25.7
			enamel	SAR-H3g			20.8	4.1	-10.9	-6.0	24.8
			enamel	SAR-H3h			17.9	3.9	-10.8	-6.7	24.0
			enamel	SAR-H3i			12.9	3.8	-10.6	-6.8	23.9
			enamel	SAR-H3j			7.7	3.5	-11.0	-6.3	24.5
			enamel	SAR-H3k			4.1	4.6	-10.7	-5.7	25.0
			cementum	SAR-H3CEM			-	6.0	-10.0	-5.0	25.7
Arbreda	Lower M3 L	A1 R-58.362	enamel	SAR-H4a	37.0		35.0	4.4	-12.4	-5.9	24.9
Alpha sector			enamel	SAR-H4b			30.6	4.1	-12.3	-5.9	24.9
Level 18			enamel	SAR-H4c			26.3	4.1	-12.2	-5.8	24.9
			enamel	SAR-H4d			23.0	4.0	-12.4	-6.2	24.5
			enamel	SAR-H4e			18.7	3.9	-12.1	-6.7	24.0
			enamel	SAR-H4f			14.5	4.4	-11.9	-6.7	24.0
			enamel	SAR-H4g			11.7	4.3	-12.2	-6.6	24.1
			enamel	SAR-H4h			8.3	4.2	-12.6	-6.3	24.5
			enamel	SAR-H4i			5.0	4.7	-12.2	-6.0	24.8
			cementum	SAR-H4CEM			-	6.3	-10.3	-5.0	25.7
Arbreda	Lower M3 R	R-69.132	enamel	SAR-H5a	48.6		45.9	4.0	-10.9	-5.7	25.0
Alpha sector			enamel	SAR-H5b			42.3	3.8	-10.8	-6.0	24.7
Level 21–24			enamel	SAR-H5c			38.0	3.8	-10.9	-5.5	25.3
			enamel	SAR-H5d			34.4	3.6	-10.8	-5.8	24.9
			enamel	SAR-H5e			30.9	3.6	-11.0	-5.2	25.6
			enamel	SAR-H5f			26.8	3.1	-11.2	-5.5	25.3
			enamel	SAR-H5g			22.2	3.6	-10.9	-4.8	26.0
			enamel	SAR-H5h			17.3	3.9	-11.0	-5.8	24.9
			enamel	SAR-H5i			12.3	3.6	-10.9	-6.4	24.3
			enamel	SAR-H5j			7.6	3.7	-10.7	-6.2	24.5
			enamel	SAR-H5k			2.8	4.1	-11.2	-6.0	24.7
			cementum	SAR-H5CEM			-	5.9	-9.6	-5.7	25.0
Arbreda	Lower M3 R	R-20.261	enamel	SAR-H6a	47.1		44.1	4.3	-11.9	-5.4	25.3
Alpha sector			enamel	SAR-H6b			40.3	3.8	-11.9	-5.5	25.2
Level 21–24			enamel	SAR-H6c			37.2	4.2	-12.0	-6.2	24.5

(*continued on next page*)

Table A1 (*continued*)

Site	Tooth	Inventory	Tissue	Lab ID	Crown height (mm)	Distance from the ERJ (mm)	Distance from the lowest crown part (mm)	CaCO3 (%)	$\delta^{13}C_{carb}$ (‰ VPDB)	$\delta^{18}O_{carb}$ (‰ VPDB)	$\delta^{18}O_{carb}$ (‰ VSMOW)
			enamel	SAR-H6d			33.1	4.4	-11.7	-6.2	24.5
			enamel	SAR-H6e			28.4	4.7	-11.9	-6.4	24.4
			enamel	SAR-H6f			24.2	4.1	-11.7	-5.5	25.2
			enamel	SAR-H6g			20.6	4.2	-11.6	-5.6	25.1
			enamel	SAR-H6h			16.4	3.6	-11.5	-6.5	24.2
			enamel	SAR-H6i			11.5	4.2	-11.6	-6.5	24.2
			enamel	SAR-H6j			8.1	4.1	-11.5	-6.0	24.7
			enamel	SAR-H6k			4.4	3.7	-11.7	-5.6	25.2
			cementum	SAR-H6CEM			-	7.0	-11.8	-5.4	25.4
Arbreda	Lower M3 R	B3 R74.236	enamel	SAR-H7a	57.0	54.6		4.2	-11.9	-4.8	26.0
Alpha sector Level 25			enamel	SAR-H7b		49.8		4.2	-12.0	-4.7	26.0
			enamel	SAR-H7c		45.5		4.0	-12.1	-4.8	25.9
			enamel	SAR-H7d		40.8		4.1	-11.7	-5.6	25.2
			enamel	SAR-H7e		36.8		3.6	-11.9	-6.4	24.3
			enamel	SAR-H7f		32.6		4.3	-11.8	-5.8	25.0
			enamel	SAR-H7g		27.9		4.4	-11.9	-5.4	25.4
			enamel	SAR-H7h		24.7		4.3	-12.0	-5.0	25.7
			enamel	SAR-H7i		22.3		4.1	-11.9	-4.6	26.1
			enamel	SAR-H7j		18.3		4.5	-11.9	-5.0	25.7
			enamel	SAR-H7k		14.2		4.3	-11.6	-5.4	25.4
			enamel	SAR-H7l		9.7		4.1	-11.9	-5.8	25.0
			enamel	SAR-H7m		7.2		3.8	-12.1	-5.2	25.6
			enamel	SAR-H7n		3.3		3.8	-11.6	-5.5	25.3
			cementum	SAR-H7CEM		-		6.0	-9.0	-4.3	26.5

Table A2

Detailed isotopic results ($\delta^{13}C_{carb}$ and $\delta^{18}O_{carb}$) for red deer teeth with incremental sampling. Underlined numbers correspond to outlier data. Brackets are added around isotopic values that are not considered reliable for further interpretation. R is for the right side, L is for the left side.

Site	Tooth	Inventory	Tissue	Lab ID	Crown height (mm)	Distance from the ERJ (mm)	Distance from the lowest crown part (mm)	CaCO3 (%)	$\delta^{13}C_{carb}$ (‰ VPDB)	$\delta^{18}O_{carb}$ (‰ VPDB)	$\delta^{18}O_{carb}$ (‰ VSMOW)
Bora Gran	Lower M3 R	BGA #1514	enamel	BOG-R1a	19.6	17.8		4.0	-9.8	-5.0	25.7
coll. Alsius			enamel	BOG-R1b		16.0		3.8	-9.5	-5.5	25.3
			enamel	BOG-R1c		12.3		4.0	-9.4	-6.0	24.8
			enamel	BOG-R1d		9.0		3.7	-9.1	-5.8	24.9
			enamel	BOG-R1e		5.8		3.9	-8.7	-6.3	24.4
			enamel	BOG-R1f		2.5		4.0	-8.8	-6.9	23.8
			dentine	BOG-R1gDEN		-		7.7	-10.2	-5.8	25.0
Bora Gran	Lower M3 R	BGA #1498	enamel	BOG-R2a	17.4	13.1		3.7	-9.8	-4.5	26.3
coll. Alsius			enamel	BOG-R2b		10.3		3.9	-9.5	-4.7	26.0
			enamel	BOG-R2c		7.3		3.8	-9.5	-5.1	25.6
			enamel	BOG-R2d		4.8		4.0	-9.8	-5.4	25.4
			enamel	BOG-R2e		3.2		4.1	-10.6	-4.5	26.3
			dentine	BOG-R2fDEN		-		7.0	-10.9	-4.8	26.0
Bora Gran	Lower M3 R	BGA #1536	enamel	BOG-R3a	25.0		21.8	broke during sampling	-	-	
coll. Alsius			enamel	BOG-R3b			17.5	3.3	-9.5	-5.3	25.5
			enamel	BOG-R3c			15.3	3.5	-9.2	-5.3	25.4
			enamel	BOG-R3d			13.1	3.5	-8.7	-5.8	24.9
			enamel	BOG-R3e			10.5	3.5	-8.6	-6.5	24.2
			enamel	BOG-R3f			7.8	3.3	-8.5	-7.3	23.4
			enamel	BOG-R3g			5.1	3.4	-8.5	-6.7	24.0
			dentine	BOG-R3hDEN			-	6.6	-9.6	-5.5	25.3
Bora Gran	Lower M3 R	BGA #1611	enamel	BOG-R4a	25.5	22.4		3.6	-10.5	-5.4	25.3
coll. Alsius			enamel	BOG-R4b		21.0		3.3	-10.4	-5.1	25.7
			enamel	BOG-R4c		17.9		3.7	-9.9	-5.7	25.1
			enamel	BOG-R4d		15.2		2.8	-10.5	-6.3	24.4
			enamel	BOG-R4e		11.8		2.8	-11.2	-5.8	24.9
			enamel	BOG-R4f		8.5		3.3	-11.2	-5.4	25.3

(*continued on next page*)

Table A2 (*continued*)

Site	Tooth	Inventory	Tissue	Lab ID	Crown height (mm)	Distance from the ERJ (mm)	Distance from the lowest crown part (mm)	CaCO3 (%)	$\delta^{13}C_{carb}$ (‰ VPDB)	$\delta^{18}O_{carb}$ (‰ VPDB)	$\delta^{18}O_{carb}$ (‰ VSMOW)
			enamel	BOG-R4g		5.1		3.8	-10.6	-5.4	25.3
			dentine	BOG-R4hDEN		-		6.4	-9.5	-4.7	26.0
Bora Gran	Lower M3 R	BGA #1543	enamel	BOG-R5a	24.5	22.4		3.3	-7.8	-5.2	25.6
coll. Alsius			enamel	BOG-R5b		18.4		3.5	-7.1	-5.7	25.1
			enamel	BOG-R5c		15.8		3.4	-6.4	-6.1	24.6
			enamel	BOG-R5d		12.4		3.4	-6.0	-6.5	24.2
			enamel	BOG-R5e		9.8		3.9	-6.5	-6.2	24.5
			enamel	BOG-R5f		5.9		3.8	-6.8	-6.0	24.7
			enamel	BOG-R5g		2.9		3.7	-7.4	-6.2	24.5
			dentine	BOG-R5hDEN		-		6.9	-8.7	-5.4	25.3
Bora Gran	Lower M3 R	BGA #1521	enamel	BOG-R6a	20.6	17.5		3.8	-10.6	-5.2	25.5
coll. Alsius			enamel	BOG-R6b		14.5		3.6	-10.7	-5.0	25.7
			enamel	BOG-R6c		11.1		3.1	-9.9	-6.9	23.8
			enamel	BOG-R6d		8.5		3.7	-9.8	-5.5	25.2
			enamel	BOG-R6e		5.3		3.4	-9.5	-6.1	24.6
			enamel	BOG-R6f		3.7		3.5	-10.0	-6.6	24.1
			dentine	BOG-R6DEN		-		5.1	-8.8	-5.4	25.3
Bora Gran	Lower M3 R	BGC #1735	enamel	BOG-RC3a	24.4	21.7		3.5	-9.5	-4.4	26.3
coll. Corominas			enamel	BOG-RC3b		18.2		3.3	-8.7	-5.4	25.4
			enamel	BOG-RC3c		15.4		3.7	-8.5	-5.4	25.3
			enamel	BOG-RC3d		11.9		3.3	-8.7	-5.5	25.2
			enamel	BOG-RC3e		9.9		3.0	-9.3	-5.1	25.7
			enamel	BOG-RC3f		6.2		3.7	-9.7	-4.2	26.6
			enamel	BOG-RC3g		2.8		3.5	-10.0	-3.5	27.3
			dentine	BOG-RC3DEN		-		6.6	-10.5	-5.1	25.6
Bora Gran	Lower M3 R	BGC #1736	enamel	BOG-RC4a	16.8	14.2		3.5	-9.5	-6.2	24.5
coll. Corominas			enamel	BOG-RC4b		12.2		3.6	-9.2	-6.6	24.1
			enamel	BOG-RC4c		10.2		3.6	-9.1	-6.0	24.7
			enamel	BOG-RC4d		7.7		3.4	-9.3	-5.4	25.4
			enamel	BOG-RC4e		4.7		3.6	-9.1	-5.8	25.0
			enamel	BOG-RC4f		2.4		3.8	-8.7	-5.3	25.5
			dentine	BOG-RC4DEN		-		6.7	-10.6	-5.9	24.8
Bora Gran	Lower M3 R	BGC #1740	enamel	BOG-RC5a	22.5	18.2		3.7	-10.0	-6.6	24.1
coll. Corominas			enamel	BOG-RC5b		15.7		3.5	-10.0	-6.3	24.5
			enamel	BOG-RC5c		13.8		3.3	-9.5	-6.5	24.2
			enamel	BOG-RC5d		11.3		3.3	-9.3	-6.9	23.8
			enamel	BOG-RC5e		7.9		3.4	-9.5	-6.9	23.8
			enamel	BOG-RC5f		5.7		3.8	-10.0	-6.1	24.6
			enamel	BOG-RC5g		2.6		3.8	-10.5	-5.3	25.5
			dentine	BOG-RC5DEN		-		6.7	-11.0	-8.4	22.3
Bora Gran	Lower M2 R	BGC #1741	enamel	BOG-RC2a	8.8		7.0	3.4	-9.7	-4.2	26.6
coll. Corominas			enamel	BOG-RC2b			4.5	3.7	-9.8	-4.1	26.7
			enamel	BOG-RC2c			2.7	3.8	-10.0	-3.6	27.2
Bora Gran	Lower M3 R	BGC #1741	enamel	BOG-RC2d	14.3		11.3	2.9	-8.1	-7.4	23.3
coll. Corominas			enamel	BOG-RC2e			8.2	2.8	-8.2	-7.4	23.3
			enamel	BOG-RC2f			5.5	3.1	-9.0	-7.5	23.2
			enamel	BOG-RC2g			3.2	3.8	-9.4	-6.6	24.1
Bora Gran	Lower M3 L	BGA #1537	enamel	BOG-R7a	22.9	19.7		3.5	-8.9	-3.6	27.2
coll. Alsius			enamel	BOG-R7b		17.8		3.7	-8.4	-3.7	27.1
			enamel	BOG-R7c		14.3		4.2	-7.9	-4.2	26.6
			enamel	BOG-R7d		11.9		4.1	-7.9	-4.7	26.0
			enamel	BOG-R7e		9.9		4.5	-8.3	-3.7	27.0
			enamel	BOG-R7f		8.0		4.1	-8.4	-4.4	26.4
			enamel	BOG-R7g		5.6		4.6	-8.4	-4.1	26.7
			enamel	BOG-R7h		3.6		4.2	-8.4	-3.4	27.4
			dentine	BOG-R7DEN		-		6.0	-9.0	-6.5	24.2
Bora Gran	Lower M3 L	BGA #1579	enamel	BOG-R8a	27.7	23.9		3.6	-9.7	-4.9	25.9
coll. Alsius			enamel	BOG-R8b		19.9		3.8	-9.3	-4.5	26.3
			enamel	BOG-R8c		17.0		3.7	-9.3	-5.5	25.2
			enamel	BOG-R8d		14.2		4.0	-9.0	-5.8	24.9
			enamel	BOG-R8e		10.2		4.1	-8.8	-6.0	24.7

(*continued on next page*)

Table A2 (*continued*)

Site	Tooth	Inventory	Tissue	Lab ID	Crown height (mm)	Distance from the ERJ (mm)	Distance from the lowest crown part (mm)	CaCO3 (%)	$\delta^{13}C_{carb}$ (‰ VPDB)	$\delta^{18}O_{carb}$ (‰ VPDB)	$\delta^{18}O_{carb}$ (‰ VSMOW)
			enamel	BOG-R8f		6.7		3.7	-9.3	-5.8	24.9
			enamel	BOG-R8g		3.5		4.3	-9.4	-5.2	25.6
			dentine	BOG-R8DEN		-		5.3	-8.4	-7.1	23.6
Bora Gran	Lower M3 L	BGA #1591	enamel	BOG-R9a	25.6	25.4		4.0	-9.5	-4.9	25.8
coll. Alsius			enamel	BOG-R9b		20.5		4.0	-8.9	-5.1	25.7
			enamel	BOG-R9c		17.7		4.3	-8.7	-6.5	24.2
			enamel	BOG-R9d		15.5		4.3	-8.7	-6.2	24.6
			enamel	BOG-R9e		12.2		4.4	-9.2	-6.0	24.7
			enamel	BOG-R9f		9.8		3.9	-9.5	-5.8	24.9
			enamel	BOG-R9g		6.0		4.3	-9.6	-5.7	25.1
			enamel	BOG-R9h		3.1		3.1	-9.6	-5.7	25.1
			dentine	BOG-R9DEN		-		5.3	-10.5	-6.6	24.1
Bora Gran	Lower M3 L	BGA #1550	enamel	BOG-R10a	17.4	15.3		4.1	-8.5	-6.7	24.0
coll. Alsius			enamel	BOG-R10b		14.0		3.6	-8.4	-6.8	23.9
			enamel	BOG-R10c		10.6		4.1	-8.6	-6.5	24.2
			enamel	BOG-R10d		8.7		4.3	-9.4	-6.7	24.0
			enamel	BOG-R10e		6.3		4.3	-9.7	-6.7	24.0
			enamel	BOG-R10f		4.1		3.9	-9.7	-6.5	24.2
			dentine	BOG-R10DEN		-		6.6	-8.8	-5.1	25.7
Bora Gran	Lower M3 L	BGA #1541	enamel	BOG-R11a	14.1	10.5		3.7	-9.1	-6.0	24.7
coll. Alsius			enamel	BOG-R11b		9.4		4.2	-9.6	-5.8	24.9
			enamel	BOG-R11c		6.9		4.1	-10.1	-5.5	25.2
			enamel	BOG-R11d		4.8		3.7	-10.4	-5.4	25.3
			enamel	BOG-R11e		2.4		3.8	-10.4	-5.5	25.3
			dentine	BOG-R11DEN		-		4.4	-9.6	-8.0	22.7
Bora Gran	Lower M2 L	BGC #1897	enamel	BOG-RC1a	16.9		15.0	2.6	-10.1	-6.0	24.7
coll. Corominas			enamel	BOG-RC1b			12.0	3.6	-9.8	-5.3	25.4
			enamel	BOG-RC1c			9.5	3.5	-10.4	-5.4	25.4
			enamel	BOG-RC1d			6.9	3.2	-10.3	-5.6	25.2
			enamel	BOG-RC1e			5.0	3.5	-10.1	-5.1	25.7
			enamel	BOG-RC1f			2.5	5.1	(-10.8)	(-5.3)	(25.4)
Bora Gran	Lower M3 L	BGC #1897	enamel	BOG-RC1g	16.6		14.5	2.9	-9.4	-5.0	25.7
coll. Corominas			enamel	BOG-RC1h			12.4	3.5	-9.8	-4.8	25.9
			enamel	BOG-RCI1i			9.7	3.7	-9.3	-4.5	26.2
			enamel	BOG-RC1j			7.5	3.4	-9.1	-4.6	26.1
			enamel	BOG-RCI1k			5.4	3.0	-8.6	-5.1	25.6
			enamel	BOG-RC1l			3.1	3.4	-9.0	-5.4	25.4
Arbreda	Lower M3 R	E0 OE69 #1628	enamel	SAR-R2a	11.8	10.32		3.4	-6.3	-6.3	24.4
Alpha sector level D			enamel	SAR-R2b		7.52		3.3	-6.5	-5.9	24.8
			enamel	SAR-R2c		5.34		3.2	-7.2	-5.3	25.4
			enamel	SAR-R2d		2.7		3.3	-7.8	-5.1	25.6
			dentine	SAR-R2eDEN		-		5.9	-9.1	-5.2	25.5
Arbreda	Lower M3 L	D5 ED14 #345	enamel	SAR-R4a	11.9	10.3		3.6	-8.5	-6.9	23.8
Alpha sector level E			enamel	SAR-R4b		8.4		3.1	-8.4	-6.5	24.2
			enamel	SAR-R4c		5.7		3.5	-9.3	-6.6	24.1
			enamel	SAR-R4d		3.4		4.2	-9.7	-5.4	25.3
			dentine	SAR-R4eDEN		-		6.1	-10.6	-5.0	25.7
Arbreda	Lower M3 L	D3 FD22 #506	enamel	SAR-R1a	21.4	19.1		3.6	-11.3	-4.5	26.3
Alpha sector level E			enamel	SAR-R1b		15.4		3.6	-10.8	-5.1	25.7
			enamel	SAR-R1c		11.8		3.9	-10.3	-6.3	24.4
			enamel	SAR-R1d		8.3		3.9	-10.3	-6.6	24.1
			enamel	SAR-R1e		6.0		4.1	-10.3	-5.7	25.1
			enamel	SAR-R1f		2.5		4.4	-10.4	-5.4	25.3
			dentine	SAR-R1gDEN		-		6.9	-10.5	-4.7	26.1
Arbreda	Lower M3 R	E3 CE116 #3182	enamel	SAR-R3a	16.0	12.6		4.0	-10.9	-5.5	25.2
Alpha sector level E			enamel	SAR-R3b		10.1		3.9	-10.9	-5.4	25.3
			enamel	SAR-R3c		7.0		3.8	-10.8	-6.0	24.7
			enamel	SAR-R3d		4.7		3.8	-10.7	-6.4	24.4
			enamel	SAR-R3e		2.4		4.4	-10.9	-6.1	24.6
			dentine	SAR-R3fDEN		-		4.8	-10.7	-6.5	24.2

Table A3

Results of elemental analysis on bone or dentine ($N_{bone\ or\ dentine}$) and collagen (C_{coll}, N_{coll}, $C{:}N_{coll}$) and of isotopic analysis on collagen ($\delta^{13}C_{coll}$, $\delta^{15}N_{coll}$) from horse (*Equus ferus*), red deer (*Cervus elaphus*) at the Serinyà caves. Underlined numbers correspond to outlier data. Brackets are added around isotopic values that are not considered reliable for further interpretation. R is for the right side, L is for the left side. * species determination confirmed by ZooMS analysis. 1: Soler and Soler, 2013; 2: Soler et al., 2014; 3: Wood et al., 2014; 4: Soler and Soler, 2016; 5: Ruff et al., 2020b; 6: Drucker et al., 2021. Tüb. stands for Tübingen and NU for National University.

Site	Lab ID	Species	Piece	Inventory	Excavation	$N_{bone\ or\ dentine}$ (%)	Yield (%)	C_{coll} (%)	N_{coll} (%)	$C{:}N_{coll}$	$\delta^{13}C_{coll}$ (‰)	$\delta^{15}N_{coll}$ (‰)	$^{13}C^{15}N$ source	$^{13}C^{15}N$ laboratory
Bora Gran	BOG-HB5	*Equus ferus*	metapodial L	Bosoms #5664	Bosoms	1.5	6.3	41.5	14.9	3.3	-20.6	7.6	this work	Tüb. Geoecology
Bora Gran	BOG-HB6	*Equus ferus**	metapodial	Bosoms #5684	Bosoms	1.5	6.7	42.2	14.6	3.4	-20.3	5.0	this work	Tüb. Geoecology
Bora Gran	BOG-HB7	*Equus ferus*	metacarpial R	Bosoms #5704	Bosoms	0.5	1.8	35.2	12.0	3.4	-21.6	3.5	this work	Tüb. Geoecology
Bora Gran	BOG-RC1	*Cervus elaphus*	jawbone L	BGA #1897	Corominas	0.3	na	na	na	na	na	na	this work	
Bora Gran	BOG-RC2	*Cervus elaphus*	jawbone R	BGA #1741	Corominas	1.5	6.5	29.8	10.7	3.2	-17.7	7.8	this work	Tüb. Geoecology
Bora Gran	BOG-R10	*Cervus elaphus*	jawbone L	BGA #1550	Alsius	0.4	1.7	<u>23.6</u>	8.6	3.2	(-20.4)	(6.9)	this work	Tüb. Geoecology
Bora Gran	BOG-R11	*Cervus elaphus*	jawbone L	BGA #1541	Alsius	0.6	2.0	39.7	14.0	3.3	-19.6	5.3	this work	Tüb. Geoecology
Bora Gran	BOG-R12	*Cervus elaphus*	metacarpial	BGA #2125	Alsius	0.2	na	na	na	na	na	na		
Bora Gran	BOG-R13	*Cervus elaphus*	metacarpial	BGA #2149	Alsius	1.0	3.7	42.0	15.0	3.3	-18.7	6.3	this work	Tüb. Geoecology
Bora Gran	BOG-R14	*Cervus elaphus*	metacarpial	BGA #2302	Alsius	1.0	4.2	42.4	14.9	3.3	-19.3	5.0	this work	Tüb. Geoecology
Bora Gran	BOG-R16	*Cervus elaphus*	metacarpial	BGA #2580	Alsius	1.0	4.9	38.4	13.7	3.3	-19.3	5.9	this work	Tüb. Geoecology
Bora Gran	BOG-R15	*Cervus elaphus**	metacarpial	BGA #2523	Alsius	0.6	3.9	36.2	12.8	3.3	-18.5	7.4	this work	Tüb. Geoecology
Arbreda	GER-1	*Cervus elaphus*	phalanx	E0 0E56 168	β, level B	nd	nd	39.8	14.9	3.1	-19.7	3.8	this work	Tüb. Geochemistry
Arbreda	GER-43	*Cervus elaphus*	phalanx	E2 B10 244	β, level C	1.5	7.1	38.2	13.3	3.3	-19.8	5.4	this work	Tüb. Geochemistry
Arbreda	GER-54	*Cervus elaphus*	1st phalanx	C3 CC12 507	β, level C	0.9	5.0	33.3	11.1	3.5	-20.1	5.2	this work	Tüb. Geochemistry
Arbreda	GER-55	*Cervus elaphus*	1st phalanx	C2 BC18 71	β, level C	1.2	4.5	30.2	10.1	3.5	-19.5	5.7	this work	Tüb. Geochemistry
Arbreda	GER-56	*Cervus elaphus*	1st phalanx	E1 DE06 551	β, level C	1.1	4.8	34.7	11.6	3.5	-20.1	5.6	this work	Tüb. Geochemistry
Arbreda	GER-3	cf *Equus ferus*	phalanx	E0 0E59 2045	β, level C	nd	nd	38.4	15.0	3.0	-21.1	3.7	this work	Tüb. Geochemistry
Arbreda	GER-44	*Equus ferus*	2nd phalanx	E2 BE6 613	β, level C	1.6	5.6	39.8	13.9	3.3	-20.9	4.7	this work	Tüb. Geochemistry
Arbreda	GER-49	*Equus ferus*	tibia R	D3 CD5 136	β, level C	0.8	3.1	35.8	12.4	3.4	-20.6	4.5	this work	Tüb. Geochemistry
Arbreda	GER-50	*Equus ferus*	tibia R	D4 DD4 328	β, level C	1.5	5.9	38.0	12.8	3.5	-20.8	4.6	this work	Tüb. Geochemistry
Arbreda	GER-51	*Equus ferus*	tibia R	D2 BD7 120	β, level C	1.6	5.9	37.9	12.6	3.5	-20.7	3.4	this work	Tüb. Geochemistry
Reclau Viver	KIA-33236	*Equus ferus**	ulna	TIII 240–270	level F	nd	nd	46.4	16.1	3.4	-20.4	4.8	this work	Tüb. Geochemistry
Arbreda	SAR-H15	*Equus ferus*	M3 upper R	E4 DE16 #219	β, level C	0.7	1.0	39.8	14.1	3.3	-21.0	7.1	this work	Tüb. Geoecology
Arbreda	SAR-H18	*Equus ferus*	M3 upper L	D3 CD11 #350	β, level C	0.9	11.6	35.4	12.8	3.2	-20.8	6.5	this work	Tüb. Geoecology
Reclau Viver	KIA-33238	*Cervus elaphus*	metapodial	TV 300–320	level D	nd	nd	44.5	15.1	3.4	-19.8	4.6	6	Tüb. Geochemistry
Reclau Viver	KIA-33243	*Cervus elaphus**	bone point	TV 350–370	level D	nd	nd	45.1	15.6	3.4	-19.5	5.0	this work	Tüb. Geochemistry
Reclau Viver	GER-9	*Cervus elaphus*	humerus L	TIII 32–340 #361	level D	1.6	6.2	42.9	14.5	3.5	-20.4	4.6	6	Tüb. Geochemistry
Reclau Viver	GER-10	*Cervus elaphus*	humerus R	TIII 32–340 #365	level D	1.0	3.0	38.5	12.9	3.5	-20.3	4.6	6	Tüb. Geochemistry
Reclau Viver	GER-11	*Cervus elaphus*	tibia R	TIII 32–340 #621	level D	1.5	6.2	43.3	14.7	3.4	-20.4	5.7	6	Tüb. Geochemistry
Reclau Viver	GER-12	*Cervus elaphus*	scapula L	TIII 32–340 #326	level D	1.0	4.0	40.6	13.8	3.4	-20.2	4.7	6	Tüb. Geochemistry
Arbreda	GER-36	*Cervus elaphus*	metapodial	E2 BE17 1787	β, level D	1.0	4.7	36.7	12.7	3.4	-20.1	4.0	6	Tüb. Geochemistry
Arbreda	GER-34	*Cervus elaphus**	skull	E2 BE14 1053	β, level D	1.2	5.6	34.7	12.2	3.3	-19.9	5.1	6	Tüb. Geochemistry
Arbreda	GER-2	*Equus ferus*	humerus	EO OE67 1475	β, level D	nd	nd	42.3	16.0	3.1	-20.8	2.6	6	Tüb. Geochemistry
Reclau Viver	GER-13	*Equus ferus*	tibia L	TIII 32–340 #364	level D	1.7	6.3	43.6	15.1	3.4	-20.7	3.2	6	Tüb. Geochemistry
Reclau Viver	GER-14	*Equus ferus*	tibia L	TIII 32–340 #700	level D	1.2	5.1	39.5	13.5	3.4	-20.8	2.7	6	Tüb. Geochemistry
Reclau Viver	GER-15	*Equus ferus*	tibia R	TIII 32–340 #573	level D	0.9	3.4	41.6	14.5	3.3	-20.6	3.3	6	Tüb. Geochemistry
Reclau Viver	GER-16	*Equus ferus**	femur L	TIII 32–340 #22	level D	0.9	3.4	40.2	14.0	3.3	-20.9	3.3	6	Tüb. Geochemistry

(*continued on next page*)

Table A3 (*continued*)

Site	Lab ID	Species	Piece	Inventory	Excavation	$N_{bone\ or\ dentine}$ (%)	Yield (%)	C_{coll} (%)	N_{coll} (%)	$C:N_{coll}$	$\delta^{13}C_{coll}$ (‰)	$\delta^{15}N_{coll}$ (‰)	$^{13}C^{15}N$ source	$^{13}C^{15}N$ laboratory
Arbreda	GER-4	*Cervus elaphus**	diaphyse	E0 0E78 2635	β, level E	nd	nd	41.8	14.9	3.3	-19.6	7.1	5	Tüb. Geoecology
Arbreda	SAR-R4	*Cervus elaphus*	jawbone L	D5 ED14 #345	β, level E	1.4	5.1	41.3	14.5	3.3	-19.1	7.0	this work	Tüb. Geoecology
Arbreda	GER-100	*Cervus elaphus*	humerus	62683	α, level 20	1.9	7.9	42.0	14.5	3.4	-20.3	7.0	5	Tüb. Geoecology
Mollet III	GER-98	cf. *Cervus elaphus*	metacarpal	N17 QN95 221	-	0.7	2.1	30.7	12.1	3.0	-20.5	5.0	this work	Tüb. Geoecology
Arbreda	ABD 2	*Cervus elaphus*	1st phalanx	E5 EE401042	β, level F	nd	nd	46.1	16.8	3.2	-20.5	7.8	3	Australian NU
Arbreda	ABD 5	cf. *Cervus elaphus*	femur R	E5 EE401046	β, level F	nd	nd	45.2	16.0	3.3	-19.2	5.1	3	Australian NU
Reclau Viver	GER-62	*Cervus elaphus*	jawbone R	F TIII 25	level A	0.8	3.5	22.5	7.9	3.3	-20.0	5.4	this work	Canada W Ontario
Reclau Viver	GER-63	*Cervus elaphus*	jawbone L	F TIII 25	level A	2.3	9.2	41.7	14.7	3.3	-19.8	5.3	this work	Canada W Ontario
Reclau Viver	GER-64	*Cervus elaphus**	metapodial	F TIII 26	level A	1.4	3.9	29.9	10.3	3.4	-19.9	4.1	this work	Canada W Ontario
Reclau Viver	GER-65	*Cervus elaphus**	2nd phalanx	F TIII 26	level A	1.3	8.4	31.0	10.8	3.3	-19.7	4.9	this work	Canada W Ontario
Reclau Viver	GER-66	*Cervus elaphus**	2nd phalanx	F TIII 26	level A	2.1	8.8	40.4	14.0	3.4	-20.1	4.9	this work	Canada W Ontario
Reclau Viver	GER-68	*Equus sp*	tibia R	F TIII 26	level A	1.3	4.8	37.0	12.8	3.4	-20.7	4.2	this work	Canada W Ontario
Reclau Viver	GER-69	*Equus sp*	tibia R	F TIII 26	level A	1.0	5.2	31.4	11.0	3.3	-20.6	3.0	this work	Canada W Ontario
Reclau Viver	GER-70	*Equus sp*	lower P2/M3	F TIII 26	level A	1.0	2.8	35.0	12.2	3.3	-20.7	5.6	this work	Canada W Ontario
Arbreda	GER-105	cf. *Equus ferus*	bone	C5 EC48 965	β, level I	0.8	5.0	33.8	11.8	3.4	-21.2	5.0	this work	Tüb. Geoecology
Arbreda	SAR-R3	*Cervus elaphus*	jawbone R	E3 CE116 3182	β, level I	2.1	10.5	45.0	15.8	3.3	-19.8	5.2	this work	Tüb. Geoecology
Arbreda	ABD 15	*Cervus elaphus*	2nd phalanx	C2 BC108 831	β, level I	nd	1.6	45.6	16.6	3.2	-19.4	3.1	3	Australian NU
Arbreda	ABD 13	*Cervus elaphus*	metatarsal R	C4 DC108 871	β, level I	nd	3.6	42.4	15.5	3.2	-20.0	4.4	3	Australian NU
Arbreda	ABD 17	*Cervus elaphus*	1st phalanx	D2 BD118 1204	β, level I	nd	1.2	47.0	16.6	3.3	-19.4	6.2	3	Australian NU
Arbreda	ABD 14	*Cervus elaphus*	1st phalanx	A5 EA112 806	β, level I	nd	1.7	46.1	16.3	3.3	-19.5	5.8	3	Australian NU

Table A4

Results of elemental analysis on bone or dentine ($N_{bone\ or\ dentine}$) and collagen (C_{coll}, N_{coll}, $C:N_{coll}$) and of isotopic analysis on collagen ($\delta^{13}C_{coll}$, $\delta^{15}N_{coll}$) from large bovids (*Bos/Bison* or likely *Bos primigenius*) and muskox (*Ovibos moschatus*) at the Serinyà caves. R is for the right side, L is for the left side. * species determination confirmed by ZooMS analysis. 1: Soler and Soler, 2013; 2: Soler et al., 2014; 3: Wood et al., 2014; 4: Soler and Soler, 2016; 5: Ruffí et al., 2020a; 6: Drucker et al., 2021. Tüb. stands for Tübingen.

Site	Lab ID	Species	Piece	Inventory	Excavation	$N_{bone\ or\ dentine}$ (%)	Yield (%)	C_{coll} (%)	N_{coll} (%)	$C:N_{coll}$	$\delta^{13}C_{coll}$ (‰)	$\delta^{15}N_{coll}$ (‰)	$^{13}C^{15}N$ source	$^{13}C^{15}N$ laboratory
Bora Gran	BOG-BB1	*Bos/Bison*	M3 lower R	Bosoms #6205	Bosoms	1.4	5.8	42.4	14.8	3.3	-18.9	7.0	this work	Tüb. Geoecology
Arbreda	GER-45	*Bos/Bison*	2nd phalanx	E2 BE7 5960	β, level C	1.1	5.3	39.7	13.9	3.3	-19.6	5.5	this work	Tüb. Geochemistry
Arbreda	GER-52	*Bos/Bison*	2nd phalanx	D3 CD 5 104	β, level C	1.6	7.5	37.6	12.7	3.5	-20.3	5.6	this work	Tüb. Geochemistry
Arbreda	GER-53	*Bos/Bison*	3rd phalanx	C4 BC3 26	β, level C	2.0	9.4	40.9	13.7	3.5	-20.4	7.0	this work	Tüb. Geochemistry
Arbreda	GER-42	*Bos/Bison**	tibia	E0 OE60 694+789	β, level C	0.6	2.1	36.5	12.8	3.3	-19.9	6.8	this work	Tüb. Geochemistry
Reclau Viver	GER-17	*Bos/Bison*	scapula R	TIII 32–340 #750	level D	2.1	7.9	43.7	15.2	3.3	-19.3	6.6	6	Tüb. Geochemistry
Reclau Viver	GER-18	*Bos/Bison*	scapula L	TIII 32–340 #743	level D	1.3	5.4	43.4	15.3	3.3	-19.4	5.9	6	Tüb. Geochemistry
Arbreda	GER-99	*Ovibos moschatus*	root M3 inf	56794	α, level 17	nd	4.5	40.2	13.8	3.4	-18.9	7.3	5	Tüb. Geoecology
Reclau Viver	GER-67	*Bos/Bison*	2nd phalanx	F TIII 26	level A	0.9	3.5	36.6	12.7	3.4	-19.8	6.3	this work	Canada W Ontario
Reclau Viver	GER-71	*Bos/Bison*	upper molar	F TIII 26	level A	0.9	3.4	25.8	8.9	3.4	-19.6	7.9	this work	Canada W Ontario
Reclau Viver	GER-72	*Bos/Bison*	astragalus	F TIII 25	level A	1.5	6.6	36.0	12.6	3.3	-19.9	9.1	this work	Canada W Ontario

Table A.5

Results of elemental analysis on collagen (C_{coll}, N_{coll}, $C:N_{coll}$) and of isotopic analysis on collagen ($\delta^{13}C_{coll}$, $\delta^{15}N_{coll}$) and radiocarbon dates (^{14}C) from horse (*Equus ferus*), red deer (*Cervus elaphus*), reindeer (*Rangifer tarandus*), muskox (*Ovibos moschatus*), rabbit (*Oryctolagus cuniculus*) and human (*Homo sapiens*) at the Serinyà caves. R is for the right side, L is for the left side. * species determination confirmed by ZooMS analysis. na stands for not applicable, nd for not determined and ind for indetermined. 1: Nadal, 1998; 2: Soler and Soler, 2013; 3: Soler et al., 2014; 4: Soler et al., 2014; 5: Wood et al., 2014; 6: Soler and Soler, 2016; 7: Ruffi et al., 2020a; 8: Soler et al., 2020b; 9: Drucker et al., 2021; 10: Soler et al., 2021.

Site	Lab ID	Species	Piece	Inventory	Excavation	Yield (%)	C_{coll} (%)	N_{coll} (%)	$C:N_{coll}$	$\delta^{13}C_{coll}$ (‰)	$\delta^{15}N_{coll}$ (‰)	Ref ^{14}C	Date ^{14}C (uncal BP)	Age range (years cal BP 2σ)	^{14}C source	$^{13}C^{15}N$ source
Bora Gran	P-7749	*Rangifer tarandus**	3rd phalanx	BGA-2222	Alsius	nd	nd	nd	nd	nd	nd	OxA-6431	12830 ± 80	15600–15090	1	na
Bora Gran	BOG-R13	*Cervus elaphus*	metacarpial	BGA-2149	Alsius	3.7	42.0	15.0	3.3	-18.7	6.3	ETH-133929	12831 ± 34	15520–15170	this work	this work
Bora Gran	BOG-R14	*Cervus elaphus*	metacarpial	BGA-2302	Alsius	4.2	42.4	14.9	3.3	-19.3	5.0	ETH-133930	12946 ± 35	15630–15310	this work	this work
Bora Gran	P-7748	cf *Rangifer tarandus*	astragalus	BGA-2153	Alsius	nd	nd	nd	nd	nd	nd	OxA-6430	13080 ± 90	15960–15360	1	na
Bora Gran	BOG-RC2	*Cervus elaphus*	jawbone R	BGA-1741	Corominas	6.5	29.8	10.7	3.2	-17.7	7.8	ETH-120651	13325 ± 38	16190–15850	this work	this work
Arbreda	GER-96	*Cervus elaphus**	lower PM3 R	G5 EG45 160	β, level A	3.9	39.3	13.9	3.3	-19.1	8.0	ETH-86105	13704 ± 41	16780–16380	10	this work
Arbreda	GER-1	*Cervus elaphus*	phalanx	E0 0E56 168	β, level B	nd	39.8	14.9	3.1	-19.7	3.8	GrA-47320	18860 ± 80	22980–22530	6	this work
Arbreda	GER-43	*Cervus elaphus*	phalanx	E2 B10 244	β, level C	7.1	38.2	13.3	3.3	-19.8	5.4	ETH-70642	19210 ± 40	23240–22960	this work	this work
Arbreda	GER-44	*Equus ferus*	2nd phalanx	E2 BE6 613	β, level C	5.6	39.8	13.9	3.3	-20.9	4.7	ETH-70643	19320 ± 45	23710–23030	this work	this work
Arbreda	GER-3	cf *Equus ferus*	phalanx	E0 0E59 2045	β, level C	nd	38.4	15.0	3.0	-21.1	3.7	GrA-47330	19480 ± 80	23770–23200	4	this work
Reclau Viver	KIA-33236	*Equus ferus**	ulna	TIII 240–270	level F	nd	46.4	16.1	3.4	-20.4	4.8	KIA-33236	19540 ± 90	23800–23250	2	this work
Arbreda	GER-41	*Oryctolagus cuniculus*	humerus	E2 BE13 1064	β, level D	6.9	38.2	13.5	3.3	-21.1	4.4	ETH-70641	18995 ± 40	23040–22870	9	9
Arbreda	Beta-521598	*Cervus elaphus*	humerus	E1 AE70 868	β, level D	nd	nd	nd	nd	nd	nd	Beta-521598	19700 ± 70	23870–23390	8	nd
Reclau Viver	KIA-33238	*Cervus elaphus*	metapodial	TV 300–320	level D	nd	44.5	15.1	3.4	-19.8	4.6	KIA-33238	19730 ± 90	23940–23370	6	9
Arbreda	GER-34	*Cervus elaphus**	skull fragment	E2 BE14 1053	β, level D	5.6	34.7	12.2	3.3	-19.9	5.1	ETH-70639	20175 ± 45	24460–23990	9	9
Reclau Viver	P-47490	*Homo sapiens*	mandible	TV 370–390, RVS-H9	level D	nd	43.0	16.2	3.1	-18.8	9.7	GrA-43815	20620 ± 80	25120–24580	9	9
Reclau Viver	KIA-33243	*Cervus elaphus**	bone point	TV 350–370	level D	nd	45.1	15.6	3.4	-19.5	5.0	KIA-33243	20830 ± 90	25350–24800	4	this work
Reclau Viver	GER-6	*Equus ferus*	scapula	TIII 280–300	level E	nd	42.0	15.5	3.2	-20.8	1.8	GrA-47352	21590 ± 90	26010–25740	4	this work
Reclau Viver	GER-13	*Equus ferus*	tibia L	TIII 32–340 #364	level D	6.3	43.6	15.1	3.4	-20.7	3.2	ETH-66711	21700 ± 70	26220–25810	9	9
Reclau Viver	GER-11	*Cervus elaphus*	tibia R	TIII 32–340 #621	level D	6.2	43.3	14.7	3.4	-20.4	5.7	ETH-70644	21720 ± 50	26060–25850	9	9
Reclau Viver	GER-8	*Homo sapiens*	femur L	TIV 330–350	level D	8.8	46.7	15.5	3.5	-20.0	10.2	ETH-66709	21900 ± 70	26360–25930	9	9
Mollet III	P-47493	*Homo sapiens*	skull	North Sector	level 4	nd	43.1	16.4	3.1	-19.3	8.7	GrA-43783	22330 ± 90	26960–26370	3	9
Arbreda	GER-2	*Equus ferus*	humerus	EO OE67 1475	β, level D	nd	42.3	16.0	3.1	-20.8	2.6	GrA-47323	22630 ± 100	27240–26450	4	9
Mollet III	GER-33	*Homo sapiens*	tibia R	M17 QM84 #54	-	3.2	42.2	15.0	3.3	-19.0	10.0	ETH-66710	22860 ± 80	27330–27070	9	9

(*continued on next page*)

Table A.5 (*continued*)

Site	Lab ID	Species	Piece	Inventory	Excavation	Yield (%)	C_{coll} (%)	N_{coll} (%)	C:N_{coll}	$\delta^{13}C_{coll}$ (‰)	$\delta^{15}N_{coll}$ (‰)	Ref^{14}C	Date^{14}C (uncal BP)	Age range (years cal BP 2σ)	^{14}C source	$^{13}C^{15}N$ source
Reclau Viver	KIA-33239	*Oryctolagus cuniculus*	tibia	TIII 360–380	level C	nd	46.6	16.1	3.4	-21.1	6.3	KIA-33239	23070 ± 120	27660–27190	3	9
Arbreda	GER-99	*Ovibos moschatus*	root M3 inf	56794	α, level 17	4.5	40.2	13.8	3.4	-18.9	7.3	ETH-93263	24530 ± 65	29010–28630	7	7
Arbreda	GrA-57326	charcoal	na	E0 0E78	β, level E	na	na	na	na	na	na	GrA-57326	24840 ± 120	29240–28790	4	na
Arbreda	ETH-100721	*Equus ferus*	femur	B5 EB10 199	β, level D	7.9	39.7	13.9	3.3	-20.6	5.2	ETH-100721	25409 ± 63	29970–29320	8	this work
Arbreda	GER-4	*Cervus elaphus**	diaphyse	E0 0E78 2635	β, level E	nd	41.8	14.9	3.3	-19.6	7.1	GrA-47351	25240 ± 120	29890–29200	4	na
Arbreda	SAR-R4	*Cervus elaphus*	jawbone L	D5 ED14 #345	β, level E	5.1	41.3	14.5	3.3	-19.1	7.0	ETH-120653	25368 ± 106	29960–29260	this work	this work
Arbreda	ABD 31	Ind.	diaphyse	E1 AE80 1301	β, level E	5.7	45.5	16.1	3.3	-20.0	7.7	OxA-21669	25780 ± 210	30740–29510	5	5
Arbreda	ABD 30	Ind.	diaphyse	E0 0E80 2945	β, level E	4.1	45.6	16.1	3.3	-20.6	4.9	OxA-21668	26100 ± 210	30870–30010	5	5
Arbreda	GER-100	*Cervus elaphus*	humerus	62683	α, level 20	7.9	42.0	14.5	3.4	-20.3	7.0	ETH-93264	26560 ± 95	31090–30430	7	7
Mollet III	GER-98	cf. *Cervus elaphus*	metacarpal	N17 QN95 221	-	2.1	30.7	12.1	3.0	-20.5	5.0	ETH-86107	28201 ± 145	32940–31780	this work	this work
Arbreda	ABD 2	*Cervus elaphus*	1st phalanx	E5 EE401042	β, level F	2.9	46.1	16.8	3.2	-20.5	7.8	OxA-21781	28260 ± 280	33260–31650	5	5
Arbreda	ABD 5	cf. *Cervus elaphus*	femur R	E5 EE401046	β, level F	3.3	45.2	16.0	3.3	-19.2	5.1	OxA-21782	28280 ± 290	33320–31640	5	5
Arbreda	ABD 6	Ind.	bone	B4 DB28643	β, level G	6.1	44.5	16.2	3.2	-19.7	3.2	OxA-21783	32100 ± 450	37610–35430	5	5
Arbreda	ABD 27	Ind.	bone	C3 CC41 1640,	β, level G	3.4	46.9	16.6	3.3	-20.8	4.6	OxA-21667	32250 ± 450	38080–35560	5	5
Arbreda	ABD 25	Ind.	bone	B2 BB36 638	β, level G	7.7	43.4	15.3	3.3	-20.4	4.3	OxA-21666	32750 ± 450	38920–36260	5	5
Arbreda	ABD 9	Ind.	bone	E0 0E110 4440	β, level H	2.5	45.3	16.5	3.2	-19.7	5.7	SANU-29014	31900 ± 530	37720–35160	5	5
Arbreda	ABD 12	Ind.	bone	E0 0E111 4484	β, level H	1.5	38.4	14.0	3.2	-19.0	9.7	SANU-29018	32100 ± 540	38230–35320	5	5
Arbreda	ABD 22	Ind.	rib	B2 BB104 1427	β, level H	3.2	43.7	15.9	3.2	-19.7	9.3	OxA-21674	33800 ± 550	40060–37090	5	5
Arbreda	ABD 10	Ind.	bone	E4 DE106 1511	β, level H	1.5	34.5	12.6	3.2	-19.8	9.0	SANU-29016	35700 ± 830	42070–39420	5	5
Arbreda	ABD 20	*Canis lupus*	radius R	E3 CE105 2771	β, level H	3.0	42.9	15.6	3.2	-18.8	10.3	OxA-21665	35850 ± 700	42020–39720	5	5
Arbreda	ABD 11	Ind.	bone	B2 BB104 1440	β, level H	1.8	44.1	16.1	3.2	-19.4	8.6	SANU-29019	35900 ± 860	42180–39550	5	5
Arbreda	ABD 18	Ind.	bone	E2 BE111 5645	β, level H	6.4	44.8	16.3	3.2	-20.7	6.0	OxA-21664	35900 ± 650	42010–39830	5	5
Arbreda	ABD 7	Ind.	bone	E3 CE108	β, level H	3.7	43.1	15.7	3.2	-18.3	6.1	OxA-21784	36000 ± 700	42090–39850	5	5
Arbreda	ABD 15	*Cervus elaphus*	2nd phalanx	C2 BC108 831	β, level I	1.6	45.6	16.6	3.2	-19.4	3.1	OxA-21663	32100 ± 450	37610–35430	5	5
Arbreda	GER-105	*Equus ferus**	bone	C5 EC48 965	β, level I	5.0	33.8	11.8	3.4	-21.2	5.0	ETH-100722	34664 ± 148	40280–39410	this work	this work
Arbreda	SAR-R3	Cervus elaphus	jawbone R	E3 CE116 #3182	β, level I	10.5	45.0	15.8	3.3	-19.8	5.2	ETH-120652	35972 ± 344	41750–40460	this work	this work

(*continued on next page*)

Table A.5 (*continued*)

Site	Lab ID	Species	Piece	Inventory	Excavation	Yield (%)	C_{coll} (%)	N_{coll} (%)	C:N_{coll}	$\delta^{13}C_{coll}$ (‰)	$\delta^{15}N_{coll}$ (‰)	Ref^{14}C	Date^{14}C (uncal BP)	Age range (years cal BP 2σ)	^{14}C source	$^{13}C^{15}N$ source
Arbreda	ABD 13	Cervus elaphus	metatarsal R	C4 DC108 871	β, level I	3.6	42.4	15.5	3.2	-20.0	4.4	OxA-21662	37300 ± 800	42730–40910	5	5
Arbreda	ABD 17	Cervus elaphus	1st phalanx	D2 BD118 1204	β, level I	1.2	47.0	16.6	3.3	-19.4	6.2	OxA-21704	39200 ± 1000	44510–42030	5	5
Arbreda	ABD 14	Cervus elaphus	1st phalanx	A5 EA112 806	β, level I	1.7	46.1	16.3	3.3	-19.5	5.8	OxA-21702	44400 ± 1900	54680–44320	5	5

Appendix B. Supporting information

Supplementary data associated with this article can be found in the online version at doi:10.1016/j.qeh.2024.100011.

References

Ackermans, N.L., Martin, L.F., Codron, D., Hummel, J., Kircher, P.R., Richter, H., Kaiser, T.M., Clauss, M., Hatt, J., 2020. Mesowear represents a lifetime signal in sheep (*Ovis aries*) within a long-term feeding experiment. Palaeogeogr. Palaeoclimatol. Palaeoecol. 553, 109793.

Alsius, P., 2015. El Magdalenense en la provincia de Gerona Vol. 1 Documenta Universitaria, Girona.

Álvarez-Lao, D.J., García, N., 2010. Chronological distribution of Pleistocene cold-adapted large mammal faunas in the Iberian Peninsula. Quat. Int. 212 (2), 120–128.

Ambrose, S.H., 1990. Preparation and characterization of bone and tooth collagen for isotopic analysis. J. Archaeol. Sci. 17 (4), 431–451.

Amundson, R., Austin, A.T., Schuur, E.A., Yoo, K., Matzek, V., Kendall, C., Uebersax, A., Brenner, D., Baisden, W.T., 2003. Global patterns of the isotopic composition of soil and plant nitrogen. Glob. Biogeochem. Cycles 17 (1).

Banks, W.E., d'Errico, F., Peterson, A.T., Vanhaeren, M., Kageyama, M., Sepulchre, P., Ramstein, G., Jost, A., Lunt, D., 2008. Human ecological niches and ranges during the LGM in Europe derived from an application of eco-cultural niche modeling. J. Archaeol. Sci. 35 (2), 481–491.

Barton, C.M., Villaverde, V., Zilhão, J., Aura, J.E., Garcia, O., Badal, E., 2013. In glacial environments beyond glacial terrains: human eco-dynamics in late Pleistocene Mediterranean Iberia. Quat. Int. 318, 53–68.

Bocherens, H., Drucker, D., Billiou, D., Moussa, I., 2005. Une nouvelle approche pour évaluer l'état de conservation de l'os et du collagène pour les mesures isotopiques (datation au radiocarbone, isotopes stables du carbone et de l'azote). l'Anthropol. 109 (3), 557–567.

Brown, W.A.B., Chapman, N.G., 1991. Age assessment of red deer (*Cervus elaphus*): from a scoring scheme based on radiographs of developing permanent molariform teeth. J. Zool. 225 (1), 85–97.

Buckley, M., Collins, M., Thomas-Oates, J., Wilson, J.C., 2009. Species identification by analysis of bone collagen using matrix-assisted laser desorption/ionisation time-of-flight mass spectrometry. Rapid Commun. Mass Sp. 23 (23), 3843–3854.

Bugalho, M.N., Milne, J.A., 2003. The composition of the diet of red deer (*Cervus elaphus*) in a Mediterranean environment: a case of summer nutritional constraint? . Ecol. Manag. 181 (1-2), 23–29.

Burjachs, F., 1993. Paleopalinología del Paleolítico Superior de la Cova de l'Arbreda (Serinyà, Catalunya). In: Fumanal, M.P., Bernabey, J. (Eds.), Estudios sobre Cuaternario. Medios sedimentarios. Cambios ambientales. Hábitat humano. Asociación Española para el Estudio del Cuaternario. Universitat de València, València, pp. 149–157.

Burjachs, F., Renault-Miskovsky, J., 1992. Paléoenvironnement et Paléoclimatologie de la Catalogne durant près de 30.000 ans (du Würmien ancien au début de l'Holocène d'après la palynologie du site de l'Arbreda (Gérone, Catalogne). Quaternaire 3 (2), 75–85.

Burke, A., Riel-Salvatore, J., Barton, C.M., 2018. Human response to habitat suitability during the Last Glacial Maximum in Western Europe. J. Quat. Sci. 33 (3), 335–345.

Cascalheira, J., Alcaraz-Castano, M., Alcolea-Gonzalez, J., de Andrés-Herrero, M., Arrizabalaga, A., Tortosa, J.E.A., Garcia-Ibaibarriaga, N., Iriarte-Chiapusso, M.J., 2021. Paleoenvironments and human adaptations during the Last Glacial Maximum in the Iberian Peninsula: a review. Quat. Int. 581, 28–51.

Cerling, T.E., Harris, J.M., 1999. Carbon isotope fractionation between diet and bioapatite in ungulate mammals and implications for ecological and paleoecological studies. Oecologia 120, 347–363.

Cerling, T.E., Harris, J.M., Ambrose, S.H., Leakey, M.G., Solounias, N., 1997. Dietary and environmental reconstruction with stable isotope analyses of herbivore tooth enamel from the Miocene locality of Fort Ternan, Kenya. J. Hum. Evol. 33 (6), 635–650.

Cole, J., 2017. Assessing the calorific significance of episodes of human cannibalism in the Palaeolithic. Sci. Rep. 7 (1), 44707.

Corominas, J.M., 1949. La Colección Corominas de la "Bora Gran". Materiales prehistóricos de Seriñá 3. Consejo Superior de Investigaciones Científicas, Zaragoza.

Craine, J.M., Elmore, A.J., Aidar, M.P., Bustamante, M., Dawson, T.E., Hobbie, E.A., Kahmen, A., Mack, M.C., McLauchlan, K.K., Michelsen, A., Nardoto, G.B., 2009. Global patterns of foliar nitrogen isotopes and their relationships with climate, mycorrhizal fungi, foliar nutrient concentrations, and nitrogen availability. N. Phytol. 183 (4), 980–992.

De Winter, N.J., Snoeck, C., Claeys, P., 2016. Seasonal cyclicity in trace elements and stable isotopes of modern horse enamel. PLoS One 11 (11), e0166678.

DeNiro, M.J., 1985. Postmortem preservation and alteration of in vivo bone collagen isotope ratios in relation to palaeodietary reconstruction. Nature 317 (6040)), 806–809.

Diefendorf, A.F., Mueller, K.E., Wing, S.L., Koch, P.L., Freeman, K.H., 2010. Global patterns in leaf ^{13}C discrimination and implications for studies of past and future climate. Proc. Natl. Acad. Sci. 107 (13), 5738–5743.

Domingo, L., Pérez-Dios, P., Fernández, M.H., Martín-Chivelet, J., Ortiz, J.E., Torres, T., 2015. Late Quaternary climatic and environmental conditions of northern Spain: An isotopic approach based on the mammalian record from La Paloma cave. Palaeogeogr. Palaeoclimatol. Palaeoecol. 440, 417–430.

Drucker, D.G., 2024. Stable isotopes and radiocarbon dating results on Late Pleistocene red deer and horse from the Serinyà caves (Girona, Catalonia, Spain) [Data set]. Zenodohttps://doi.org/10.5281/zenodo.11108332

Drucker, D.G., Bridault, A., Hobson, K.A., Szuma, E., Bocherens, H., 2008. Can carbon-13 in large herbivores reflect the canopy effect in temperate and boreal ecosystems? Evidence from modern and ancient ungulates. Palaeogeogr. Palaeoclimatol. Palaeoecol. 266 (1-2), 69–82.
Drucker, D.G., Hobson, K.A., Ouellet, J.P., Courtois, R., 2010. Influence of forage preferences and habitat use on ^{13}C and ^{15}N abundance in wild caribou (*Rangifer tarandus caribou*) and moose (*Alces alces*) from Canada. Isot. Environ. Health Stud. 46 (1), 107–121.
Drucker, D.G., Naito, Y.I., Coromina, N., Rufí, I., Soler, N., Soler, J., 2021. Stable isotope evidence of human diet in Mediterranean context during the Last Glacial Maximum. J. Hum. Evol. 154, 102967.
Fernández-García, M., López-García, J.M., Lorenzo, C., 2016. Palaeoecological implications of rodents as proxies for the Late Pleistocene–Holocene environmental and climatic changes in northeastern Iberia. Comptes Rendus Palevol 15 (6), 707–719.
Fernández-García, M., Pederzani, S., Britton, K., Agudo-Pérez, L., Cicero, A., Geiling, J., Daura, J., Sanz-Borrás, M., Marín-Arroyo, A.B., 2023. Ecological evolution in northern Iberia (SW Europe) during the Late Pleistocene through isotopic analysis on ungulate teeth. Biogeosci. Discuss. 1–44.
Fortelius, M., Solounias, N., 2000. Functional characterization of ungulate molars using the abrasion-attrition wear gradient: a new method for reconstructing paleodiets. Am. Mus. Novit. 3301, 1–36.
Fricke, H.C., Clyde, W.C., O'Neil, J.R., 1998. Intra-tooth variations in $\delta^{18}O$ (PO4) of mammalian tooth enamel as a record of seasonal variations in continental climate variables. Geochim. Cosmochim. Acta 62 (11), 1839–1850.
Fu, Q., et al., 2016. The genetic history of ice age Europe. Nature 534 (7606)), 200–205.
Garcia-Guixé, E., Martínez-Moreno, J., Mora, R., Núñez, M., Richards, M.P., 2009. Stable isotope analysis of human and animal remains from the Late Upper Palaeolithic site of Balma Guilanyà, southeastern Pre-Pyrenees, Spain. J. Archaeol. Sci. 36 (4), 1018–1026.
Grine, F.E., 1986. Dental evidence for dietary differences in *Australopithecus* and *Paranthropus*: a quantitative analysis of permanent molar microwear. J. Hum. Evol. 15, 783–822.
Guiry, E.J., Szpak, P., 2021. Improved quality control criteria for stable carbon and nitrogen isotope measurements of ancient bone collagen. J. Archaeol. Sci. 132, 105416.
Harlé, E., 1882. La grotte de Serinyà, près de Gérone (Espagne). Matériaux pour l'histoire primitive et naturelle. De. l'Homme 13, 293–299.
Heaton, T.H., 1999. Spatial, species, and temporal variations in the 13C/12C ratios of C3 plants: implications for palaeodiet studies. J. Archaeol. Sci. 26 (6), 637–649.
Hedges, R.E., 2003. On bone collagen—apatite-carbonate isotopic relationships. Int. J. Osteoarchaeol. 13 (1-2), 66–79.
Höbig, N., et al., 2012. Lake Banyoles (northeastern Spain): a Last Glacial to Holocene multi-proxy study with regard to environmental variability and human occupation. Quat. Int. 274, 205–218.
Högberg, P., 1997. 15N natural abundance in soil–plant systems. N. Phytol. 137 (2), 179–203.
Hoppe, K.A., Stover, S.M., Pascoe, J.R., Amundson, R., 2004. Tooth enamel biomineralization in extant horses: implications for isotopic microsampling. Palaeogeogr. Palaeoclimatol. Palaeoecol. 206 (3-4), 355–365.
Hughes, P.D., Gibbard, P.L., 2015. A stratigraphical basis for the Last Glacial Maximum (LGM). Quat. Int. 383, 174–185.
Jones, J.R., Marín-Arroyo, A.B., Straus, L.G., Richards, M.P., 2020. Adaptability, resilience and environmental buffering in European Refugia during the Late Pleistocene: Insights from La Riera cave (Asturias, cantabria, Spain). Sci. Rep. 10 (1), 1217.
Jones, J.R., Richards, M.P., Reade, H., de Quirós, F.B., Marín-Arroyo, A.B., 2019. Multi-Isotope investigations of ungulate bones and teeth from El Castillo and Covalejos caves (Cantabria, Spain): Implications for paleoenvironment reconstructions across the Middle-Upper Palaeolithic transition. J. Archaeol. Sci. Rep. 23, 1029–1042.
King, T., Andrews, P., Boz, B., 1999. Effect of taphonomic processes on dental microwear. Am. J. Phys. Anthropol. 108, 359–373.
Koch, P.L., Tuross, N., Fogel, M.L., 1997. The effects of sample treatment and diagenesis on the isotopic integrity of carbonate in biogenic hydroxylapatite. J. Archaeol. Sci. 24 (5), 417–429.
Kohn, M.J., 2010. Carbon isotope compositions of terrestrial C3 plants as indicators of (paleo) ecology and (paleo) climate. Proc. Natl. Acad. Sci. 107 (46), 19691–19695.
Kohn, M.J., Cerling, T.E., 2002. Stable isotope compositions of biological apatite. Rev. Mineral. Geochem. 48 (1), 455–488.
Kohn, M.J., Schoeninger, M.J., Valley, J.W., 1996. Herbivore tooth oxygen isotope compositions: effects of diet and physiology. Geochim. Cosmochim. Acta 60 (20), 3889–3896.
Levin, N.E., Cerling, T.E., Passey, B.H., Harris, J.M., Ehleringer, J.R., 2006. A stable isotope aridity index for terrestrial environments. Proc. Natl. Acad. Sci. 103 (30), 11201–11205.
Lloveras, L., Garcia, L., Marqueta, M., Maroto, J., Soler, J., Soler, N., 2022. The role of birds in Upper Palaeolithic sites: Zooarchaeological and taphonomic analysis of the avian remains from Arbreda Cave (Serinyà, northeast Iberia). Quat. Int. 626, 22–32.
Longin, R., 1971. New method of collagen extraction for radiocarbon dating. Nature 230 (5291), 241–242.
Longinelli, A., 1984. Oxygen isotopes in mammal bone phosphate: a new tool for paleohydrological and paleoclimatological research? Geochim. Cosmochim. Acta 48 (2), 385–390.
López-García, J.M., Soler, N., Maroto, J., Soler, J., Alcalde, G., Galobart, À., Bennàsar, M., Burjachs, F., 2015. Palaeoenvironmental and palaeoclimatic reconstruction of the Latest Pleistocene of L'Arbreda Cave (Serinyà, Girona, northeastern Iberia) inferred from the small-mammal (insectivore and rodent) assemblages. Palaeogeogr. Palaeoclimatol. Palaeoecol. 435, 244–253.
Lowe, J.J., Rasmussen, S.O., Björck, S., Hoek, W.Z., Steffensen, J.P., Walker, M.J., Yu, Z.C., Intimate Group, 2008. Synchronisation of palaeoenvironmental events in the North Atlantic region during the Last Termination: a revised protocol recommended by the INTIMATE group. Quat. Sci. Rev. 27 (1-2), 6–17.
Margari, V., Hodell, D.A., Parfitt, S.A., Ashton, N.M., Grimalt, J.O., Kim, H., Yun, K.S., Gibbard, P.L., Stringer, C.B., Timmermann, A., Tzedakis, P.C., 2023. Extreme glacial cooling likely led to hominin depopulation of Europe in the Early Pleistocene. Science 381 (6658)), 693–699.
Maroto, J., 2014. Localities of Reclau. In: Sala Ramos, R., Carbonell, E., Bermúdez de Castro, J.M., Arsuaga, J.L. (Eds.), Pleistocene and Holocene Hunter-gatherers in Iberia and the Gibraltar Strait: the current archaeological record. Universidad de Burgos, Fundación Atapuerca, Burgos, pp. 247–255.
Michelsen, A., Schmidt, I.K., Jonasson, S., Quarmby, C., Sleep, D., 1996. Leaf 15N abundance of subarctic plants provides field evidence that ericoid, ectomycorrhizal and non-and arbuscular mycorrhizal species access different sources of soil nitrogen. Oecologia 105, 53–63.
Micó, C., Blasco, R., Muñoz Del Pozo, A., Jiménez-García, B., Rosell, J., Rivals, F., 2024. Differentiating taphonomic features from trampling and dietary microwear, an experimental approach. Hist. Biol. 36 (4), 760–782.
Mihlbachler, M.C., Rivals, F., Solounias, N., Semprebon, G.M., 2011. Dietary change and evolution of horses in North America. Science 331, 1178–1181.
Nadal, J., 1998. Les faunes del Plistocè final-Holocè a la Catalunya Meridional i de Ponent. Interpetacions tafonòmiques i paleoculturals. Ph.D. Thesis, Universitat de Barcelona, Spain.
Pèrez-Obiol, R., Julià, R., 1994. Climatic change on the Iberian Peninsula recorded in a 30,000-yr pollen record from Lake Banyoles. Quat. Res. 41 (1), 91–98.
Pericot, L., 1945. Nuevos descubrimientos Paleolíticos en Cataluña. Arch. De. Prehist. Levant. 2, 337–339.
Pericot, L., Maluquer, J., 1951. La colección Bosoms. Materiales prehistóricos de Seriñá 2. Consejo Superior de Investigaciones Científicas, Zaragoza.
Posth, C., et al., 2023. Palaeogenomics of upper palaeolithic to neolithic European hunter-gatherers. Nature 615, 117–126.
Ramsey, C.B., Lee, S., 2013. Recent and planned developments of the program OxCal. Radiocarbon 55 (2), 720–730.
Reimer, P.J., Austin, W.E., Bard, E., Bayliss, A., Blackwell, P.G., Ramsey, C.B., Butzin, M., Cheng, H., Edwards, R.L., Friedrich, M., Grootes, P.M., 2020. The IntCal20 Northern Hemisphere radiocarbon age calibration curve (0–55 cal kBP). Radiocarbon 62 (4), 725–757.
Revelles, J., Allue, E., Alcolea, M., Antolin, F., Berihuete-Azorin, M., Exposito, I., Garay, B., Mas, B., Pique, R., Obea, L., Val-Peon, C., 2022. Site formation processes, human activities and palaeoenvironmental reconstructions from archaeobotanical records in cave and rock-shelter sites in NE Iberia. Rev. Palaeobot. Palynol. 299, 104612.
Rink, W.J., Schwarcz, H.P., 1995. Tests for diagenesis in tooth enamel: ESR dating signals and carbonate contents. J. Archaeol. Sci. 22 (2), 251–255.
Rivals, F., 2019. MicrowearBivaR: a code to create tooth microwear bivariate plots in R (Version 1). Zenodo. https://doi.org/10.5281/zenodo.2587575
Rivals, F., 2024. Dental raw mesowear and microwear data for *Equus ferus* and *Cervus elaphus* from Abreda Cave (levels D-I) and Bora Gran (Spain) [Data set]. Zenodo. https://doi.org/10.5281/zenodo.10961000
Rivals, F., Mihlbachler, M.C., Solounias, N., 2007. Effect of ontogenetic-age distribution in fossil samples on the interpretation of ungulate paleodiets using the mesowear method. J. Vertebr. Paleontol. 27, 763–767.
Rufí, I., Drucker, D.G., Bocherens, H., Lloveras, L., Madurell-Malapeira, J., Maroto, J., Soler, J., Soler, N., 2020a. Revision of the occurrence of muskox (*Ovibos moschatus* Zimmermann 1780) from the Gravettian of Arbreda Cave (Serinyà, northeastern Iberian Peninsula): new insights for the study of Iberian cold-adapted faunas. Boreas 49 (4), 858–872.
Rufí, I., Lloveras, L., Soler, J., Soler, N., 2019. Subsistence strategies of Gravettian hunter–gatherers in the northeast of the Iberian Peninsula: the case of level E of Arbreda Cave (Serinyà). Archaeol. Anthropol. Sci. 11, 6663–6688.
Rufí, I., Lloveras, L., Soler, J., Soler, N., 2020b. Small prey exploitation during the final Gravettian in the northeast of the Iberian Peninsula: the case of Level D from Arbreda Cave. Int. J. Osteoarchaeol. 30 (3), 330–344.
Rufí, I., Lloveras, L., Soler, J., Soler, N., 2021. Subsistence practices in western Mediterranean Europe during the Final Gravettian. Zooarchaeological and taphonomic analysis of faunal remains from level D of Arbreda Cave (Serinya, NE Iberian Peninsula). J. Quat. Sci. 36 (3), 467–487.
Sánchez-Hernández, C., Gourichon, L., Soler, J., Soler, N., Blasco, R., Rosell, J., Rivals, F., 2020. Dietary traits of ungulates in northeastern Iberian Peninsula: Did these Neanderthal preys show adaptive behaviour to local habitats during the Middle Palaeolithic? Quat. Int. 557, 47–62.
Soler, N., 1976. La Bora Gran d'en Carreres, in: Canal, J., Soler, N.(Eds.), El Paleolític a les Comarques Gironines. Servei d'Investigacions Arqueològiques, Girona, pp. 156–157.
Soler, N., 1999. Le Paléolithique des grottes de Serinyà (Gérone, Catalogne, Espagne), in: Sacchi, D. (Ed.), Les faciès leptolithiques de nord-ouest méditerranéen: milieux naturels et culturels. Société Préhistorique Française et Ministère de la Culture, Carcassonne, pp.195–228.
Soler, J., Soler, N., Agustí, B., Bolus, M., 2013. The Gravettian calvaria from Mollet III cave (Serinyà, Northeastern Iberian Peninsula). J. Hum. Evol. 65, 322–329.
Soler, J., Soler, N., Rufí, I., Niell, X., Masclans, A., Coromina, N., Solés, A., Ventura, H., 2021. El Magdaleniense en la cueva de la Arbreda (Serinyà, Pla de l'Estany, Cataluña). In: Bea, M., Domingo, R., Mazo, C., Montes, L., Rodanés, J.M. (Eds.), De la mano de la Prehistoria. Homenaje a Pilar Utrilla Miranda. Monografías Arqueológicas, Prehistoria 57. Prensas de la Universidad de Zaragoza, Zaragoza, pp. 309–324.
Soler, J., Soler, N., Solés, A., Niell, X., 2014. Cova de l'Arbreda from the Middle Paleolithic to the Neolithic. In: Sala Ramos, R., Carbonell, E., Bermúdez de Castro, J.M., Arsuaga, J.L. (Eds.), Pleistocene and Holocene Hunter-Gatherers in Iberia and the Gibraltar Strait: the current archaeological record. Universidad de Burgos, Fundación Atapuerca, Burgos, pp. 266–276.

Soler, N., Soler, J., 2013. Cabezas de fémur de ciervo perforadas en la cueva del Reclau Viver (Serinyà, Girona) y el Gravetiense final en el norte de Cataluña, in: de la Rasilla Vives M. (Ed.), Estudios en homenaje Francisco Javier Fortea Pérez. Universitatis Ovetensis Magister. Ediciones de la Universidad de Oviedo, Oviedo, pp. 317–334.

Soler, N., Soler, J., 2016. The first *Homo sapiens* in Catalonia, hunters and gatherers from the old Upper Palaeolithic. Catalan Hist. Rev. 9, 9–23.

Solounias, N., Semprebon, G., 2002. Advances in the reconstruction of ungulate ecomorphology with application to early fossil equids. Am. Mus. Novit. 3366, 1–49.

Sommer, R.S., Nadachowski, A., 2006. Glacial refugia of mammals in Europe: evidence from fossil records. Mam. Rev. 36 (4), 251–265.

Sponheimer, M., Lee-Thorp, J.A., 1999. Oxygen isotopes in enamel carbonate and their ecological significance. J. Archaeol. Sci. 26 (6), 723–728.

Stephens, R.B., Ouimette, A.P., Hobbie, E.A., Rowe, R.J., 2022. Reevaluating trophic discrimination factors ($\Delta\delta^{13}C$ and $\Delta\delta^{15}N$) for diet reconstruction. Ecol. Monogr. 92 (3), e1525.

Stevens, R.E., Balasse, M., O'Connell, T.C., 2011. Intra-tooth oxygen isotope variation in a known population of red deer: implications for past climate and seasonality reconstructions. Palaeogeogr. Palaeoclimatol. Palaeoecol. 301 (1-4), 64–74.

Stewart, J.R., Lister, A.M., Barnes, I., Dalén, L., 2010. Refugia revisited: individualistic responses of species in space and time. Proc. R. Soc. B 277 (1682), 661–671.

Straus, L.G., 2013. Iberian archaeofaunas and hominin subsistence during Marine Isotope Stages 4 and 3. Zooarchaeology Mod. Hum. Orig.: Hum. Hunt. Behav. later Pleistocene 97–128.

Straus, L.G., Bicho, N., Winegardner, A.C., 2000. The Upper Palaeolithic settlement of Iberia: first-generation maps. Antiquity 74 (285), 553–566.

Svenning, J.C., Normand, S., Kageyama, M., 2008. Glacial refugia of temperate trees in Europe: insights from species distribution modelling. J. Ecol. 96 (6), 1117–1127.

Tejada-Lara, J.V., MacFadden, B.J., Bermudez, L., Rojas, G., Salas-Gismondi, R., Flynn, J.J., 2018. Body mass predicts isotope enrichment in herbivorous mammals. Proc. R. Soc. B 285 (1881), 20181020.

Uzunidis, A., Pineda, A., Jiménez-Manchón, S., Xafis, A., Ollivier, V., Rivals, F., 2021. The impact of sediment abrasion on tooth microwear analysis: an experimental study. Archaeol. Anthropol. Sci. 13, 134.

Van der Plicht, J., Palstra, S.W.L., 2016. Radiocarbon and mammoth bones: what's in a date. Quat. Int. 406, 246–251.

Van Klinken, G.J., 1999. Bone collagen quality indicators for palaeodietary and radiocarbon measurements. J. Archaeol. Sci. 26 (6), 687–695.

Vegas-Vilarrúbia, T., et al., 2013. Diatom and vegetation responses to Late glacial and early Holocene climate changes at Lake Estanya (southern Pyrenees, NE Spain). Palaeogeogr. Palaeoclimatol. Palaeoecol. 392, 335–349.

Wood, R.E., Arrizabalaga, A., Camps, M., Fallon, S., Iriarte-Chiapusso, M.J., Jones, R., Maroto, J., De la Rasilla, M., Santamaría, D., Soler, J., Soler, N., 2014. The chronology of the earliest Upper Palaeolithic in northern Iberia: new insights from L'Arbreda, Labeko Koba and La Viña. J. Hum. Evol. 69, 91–109.

Zazzo, A., Balasse, M., Patterson, W.P., 2005. High-resolution δ13C intratooth profiles in bovine enamel: Implications for mineralization pattern and isotopic attenuation. Geochim. Cosmochim. Acta 69 (14), 3631–3642.

Zazzo, A., Balasse, M., Patterson, W.P., 2006. The reconstruction of mammal individual history: refining high-resolution isotope record in bovine tooth dentine. J. Archaeol. Sci. 33 (8), 1177–1187.